Response to Anonymous Referee#1

First we would like to thank Referee#1 for taking the time to review our paper. We appreciated your comments that have helped to clarify and improve our paper. We will address your comments in the order of the review below

First to address the general comments:

1) Validation of the assumption of July 1 Layer age as melt can continue into August.
Yes we realize that melt can continue into August; however the majority of the warm temperatures are in late june and early july. The radar will cause the largest reflection where the density change is largest and hence we chose July 1 as this date. Early and late season melt event could cause a thin layer to form but it would not be the dominate peak in the radar return which would be caused by the larger summer-time densification. This same argument holds for hoar layers in the interior. Again we add a +/- one month error on this data to show the uncertainly as stated in section 4.2.

2) Conveying more detail on the MAR density model.- We have included the basic equation of the density model now in Section 3.2 for more clarity. Additionally we understand the reviewer was confused by how we were conducting our density comparison as we did leave out a very important sentence clarifying that our modeled and measured density profile were compared simultaneously in time. In Section 4.1 this sentence was added, "The comparison of measured and modeled density was simultaneous in time, meaning that the MAR density profile output on the day of the measurement was compared to the measurement."

3) More appropriate cross over analysis comparing range bins-

This has been changed to include both range bins and m w.e.

4) An improvement to the uncertainty analysis and description.
We have added some clarification to Section 4.2 and below are calculations our calculations for the reviewer. First we have both correlated and uncorrelated errors as the density error is correlated. We take the now equation 3 and take the derivative as follows.

$$b = \frac{A\rho}{(\rho D+1)^{1.5}} \quad \text{where } A = \frac{TWT(x)\cdot c}{2a(x)\rho_w}$$

$$\frac{\partial b}{\partial \rho} = \frac{A}{(\rho D+1)^{1.5}} + \frac{-1.5A\rho}{(\rho D+1)^{2.5}}$$

Taylor Series: to account for error, $\Delta\rho$,

$$b_{error} \cong \frac{A\rho}{(\rho D+1)^{1.5}} + \underbrace{\Delta_\rho \cdot \left[\frac{A}{(\rho D+1)^{1.5}} + \frac{-1.5A\rho}{(\rho D+1)^{2.5}}\right]}_{\text{error term } \Delta_b}$$

$$\frac{\Delta b}{b} = \frac{\Delta\rho}{\rho} + \frac{-1.5\Delta\rho}{(\rho D+1)}$$

$$= \frac{\Delta\rho}{\rho}\left[1 + \frac{-1.5\rho}{\rho D+1}\right] //$$

where $D = \frac{\epsilon_i^{1/3}-1}{\rho_{ice}}$. This equation relates % error in $\Delta\rho$ (i.e. $\frac{\Delta\rho}{\rho}$) with % error in b.

So the % error in accumulation has a scale factor that depends on density. The scale factors dependence on density is as follows.

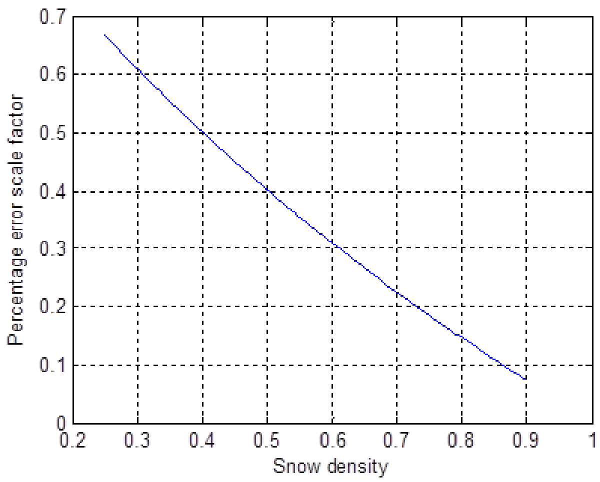


```
D = (3.15^(1/3) - 1)/0.917;
rho = linspace(0.25,1,101);
plot(rho,(1 - 1.5*rho./(rho*D+1)))
```

We choose the highest Percent error scale for our density measurements that rarely go below 0.3 giving a percentage error scale of 0.6.
Using sum of squares on uncorrelated density (12%* scale factor of 0.6) error to age (8%) error
We get sqrt((12*0.6)^2 + 8^2) = 10.76 which we round to an error of 11%. If we assume the maximum age error of 10% as suggested by the reviewer. We get sqrt((12*0.6)^2 + 10^2) = 12.32 or 12%. We have changed the error to the higher error of 12% to stratify the reviewer and added clarifying statements in Section 4.2.

Specific Comments	**Response**
Justify comparing radar-derived and in situ measurements that are within 5 km of each other	Yes we realize accumulation can change on small scales, as shown by the ice cores in figure 12. Determining correlation length scales would vary considerable depending on the ice sheet region. While this could be

	done with our dataset it would be a very detailed study and beyond the scope of this paper. We choose 5 km as a scale that provided a few (2) locations where we have both radar-derived and in situ measurements in relatively close proximity and in time. Choosing a smaller number like (1km) would only allow for overlap at 1 location. This is similar to other studies where ice cores are extrapolated over space to validate model e.g. Colgan et al., 2015. We realize it would be best to have ice cores directly under all IceBridge flight lines simultaneous in time but in reality few exist, hence, we set the distance at 5 km for this study.
Density comparison- Model evaluation	We have added additional equations and clarifications in sections 3.2 and 4.1. Again we are comparing SUMup Measurements on the date they were taken with the same profile date in MAR. If only a month was given we use the 1st of the month for comparison. We also state clearly in this paper in Section 4.1 that "We consider it beyond the scope of this study to investigate and explain why MAR underestimates near-surface density, therefore, here we assume that the firn density in the top 1 m is 0.338 g cm^{-3}. " The reviewer is correct that much more needs to be done in understanding why the density model is not producing similar results to measurements in the top 1 m and Co Author Alexander is working on this exact problem for his post doctoral project and will be publishing more detailed results shortly.
Radar collection date to MAR density	In Section 4.1 we now clarify this with "the spatially-varying modelled density profiles are used for April 30"

<table>
<tr>
<td></td>
<td>We are use density profiles from April 30 to calculate accumulation form the radar data which is approximately the mid-point for IceBridge flights.

We also note that in the MAR model during the spring time frame our choice of date would have little impact as shown in the table below for the different dates compared to the observed values from the PARCA cores.

<table>
<tr><th></th><th>Observed</th><th>MAR
(Apr 15)</th><th>MAR
(May 1)</th><th>MAR
(May 15)</th><th>MAR
(June 1)</th></tr>
<tr><td>0-1 m</td><td>338 ± 39</td><td>282 ± 40</td><td>280 ± 40</td><td>275 ± 45</td><td>277 ±52</td></tr>
<tr><td>1 – 2.5 m</td><td>381 ± 54</td><td>385±149</td><td>387 ± 149</td><td>386 ± 148</td><td>390 ± 148</td></tr>
</table>
</td>
</tr>
<tr>
<td>Constant Density Assumption</td>
<td>Additional discussion is added in section 6, however, we note that the SUMup compilation of field measurements does not support the reviewer claim that surface densities should very by up to 30%. It is very rare to have surface measurement below 300 kg/m3 for Greenland. SUMup measurements, the largest compilation of publically available measurements that we are aware of, which are well distributed spatially on the GrIS (Figure 1) show a spatial variability of ~20% (12% std) spatially. In the paper we clearly state the assumption made and cannot address the spatial bias until models and measurements are in better agreement.</td>
</tr>
<tr>
<td>Accumulation rates and uncertainties : Age of first layer</td>
<td>This is defined in Section 5.1 the second paragraph and we added "We simultaneously compare the time represent by the layer to MAR estimates of accumulation." For clarification</td>
</tr>
</table>

Error Estimate	This is addressed in the opening comments.
Picking procedures. Smoothing.	We have added clarification to this section and Figure 3 is included. Changed smoothing to spline fitted for clarity. The data is not smoothed.
Results: Time frame	We went through results to make sure it was clear what time frame was represented as well as added time ranges to figure captions etc as suggested.
Annual Variations	Snow radar has previous been shown to detect annual layers (Medley et al., 2013 published by this journal) The layers here are annual as variation and not monthly variations as suggested due to the magnitude of the change. Shown in Figure
First layer	We chose to keep the analysis of the first layer. We provide the uncertainty estimates and the first layer is the most extensive across the ice sheet. Again we are comparing the 10 months represented by this layer to 10 months of modeled data so the comparison is valid.
Crossover Analysis	Included Range bins and clarifications as suggested. We do not do cross over analysis of deeper layers and there are not many locations to perform this analysis as Shown in Figure 6.
Comparison with model	Language has been toned down as suggested. We note again that the measured densities show less of a regional bias than the modeled densities so we would expect that using the average value decreases spatial bias over modeled values. We have clarified dates throughout as suggested.
Comparison with in situ data	We chose not to include the echograms we are using

	the pick at the closest radar trace for this analysis.
Discussion	We have added some to the Discussion but do not extrapolate to Greenland mass balance as that is future work. This paper is as the review suggests and introduction to this dataset and the description of how it was created with a preliminary comparison to MAR. Future work will expand its use.
Technical Corrections	
P: 6699 L20: remove “of ice” as it is implied L23: remove “being governed by” and “being dominated by” as it is redundant and awkward	Changed.
P: 6700 L3: “here after” should be “hereafter” L6: add “in number” after “limited” to clarify L11: comma after “(Benson, 1962)” L27: replace “and map” with “the lateral persistence of”	Changed.
P: 6701 L8: use of “to” after “penetrate” is redundant; consider removing “to” or rephrasing L10: comma after “frequency-modulated” L11: remove the comma after “radars” L25: comma after “preserved” and remove the	Changed

commas around ", therefore," or consider a semicolon after "preserved" and remove "and"	
P: 6702 L16: comma after "Frequency-Modulated" ; also, I am not sure why "Frequency-Modulated Continuous Wave" is capitalized here and not on P6701, L10- 11, so please be consistent. I suggest not capitalizing it. L17: change "when preserved" to "where preserved" Section 3.1: somewhere in this section there should be a description of the differences in the radar system for the different years, including its range precision.	Change, made consistent, range resolution is given in Section 3.1. We chose not to describe the radar changes here as they are given in the citations and not relevant to the work done in this paper. Additionally the radar changes are minor over this time period.
P: 6703 L3-4: remove "reanalysis" add "global atmospheric reanalysis" after "ERAInterim" L12: change "accumulation-rate" to "accumulation rates" as the former suggests you are using accumulation rate profiles from MAR, which seems awkwardly	Changed. To a depth of 15 m is clarified with the parenthetical information given in the paper (the depth to which MAR predicts firn densities). We clarified the sentence on the number of measurements and information and Figure 1 shows the number of locations. Changed sentence to: "which contains over 1500 measurements from snow pits and ice cores at 62 sites. At each site the number of measurements ranges in number between 8 and 170 and maximum depths of 1 m to 15 m."

phrased L20: Why only to 15 m? Is it due to the fact that no layers below 15 m are used? If so, please state it. L20: “1500 measurements” is misleading and really does not inform the reader of the value of the data set for comparison. I would prefer listing the number of sites, with a description of the range of measurements at each site. Something along the lines of “which contains measurements at ## sites, and at each site the number of measurements ranges in number between XX and XX and maximum depths of XX and XX.” L23: change “measured” to “in situ” L26: change “additionally” to “additional” L27: The phrase “which includes additional cores to the SUMup dataset” is redundant because it was already made clear by the “additional” in the prior line.	
P6704 L5: The second half of	Change to “Because we seek to derive accumulation

the sentence is oddly phrased, please reword beginning at “we require: : :” L18-19: The sentence beginning with “We note: : :” needs to be appropriately cited as this is not common knowledge.	rates from near-surface radars across large portions of the ice sheet, we require firn density profiles that cover the GrIS.” For clarity. Change to “Uncertainty in the top meter is assigned by the ±1σ variation in observed density (12%) which we assume is due to the natural variability in surface density.”
P6705 L1-2: in the sources of error for derivation of radar depth, why is the actual density profile used not included in the list? The error from uncertainty in density is likely larger than based on the dielectric model used. L2-6: The description of the dielectric model evaluation is confusing, please clarify. Perhaps, begin with a statement explaining that you are evaluating X, Y, Z dielectric models because that only became apparent at the end. Eq1: Why is a dependent on x? The age of a layer should not be dependent on location as	We choose not to add additional information on the dielectric models as we feel it is clear the models that were used from the references and the main point that there can be up to a 3% error is stated clearly. WE have rewriting previous eq 1 into Equations 1 through 3 for clarity please see section 4.2 as it has been undergone many changes for clarity. Added average.

the layers are assumed isochronous. The equation might need further clarification because variables should be dependent on x, but also on depth (or on the layer number). I suggest stating the equation is for a given horizon to eliminate the additional complexity. L13: The phrase ": : : is cumulated snow/firn density at depth: : :" is confusing. I suggest adding "average" after "cumulated" because otherwise it sounds as if the densities are just added together. L16: The same issue arises here as with the previous comment. The use of "cumulative" suggests adding together all the densities below that depth, which in an integrative sense would produce a cumulative mass (kg m-2). Perhaps, reword or add "average" again.	
P6707 L2-3: If vertical traces	The stacking procedure is described a few lines down

are tossed out if it appears the surface is not properly picked, how is the stacking procedure done? If a few traces in a row are tossed out, you would not want to average the now spatially separated traces. L7-8: Why not stack a different number of traces to end up with similar along-track spacing for all years? L13: change "in" to "from" L24-26: please rephrase the sentence beginning with "Layer indices are: : :" because I find it difficult to understand what is meant by the "partial overlap that can exist between layers." A graphic of the procedure is really necessary.	with "The radar data are then horizontally averaged (stacked) 10 times to an along-track spacing of ~50 m, in 2011 and 2012, and ~10 m, in 2009 and 2010" Yes vertical traces are removed because the surface is not always pick correctly. This common with radar data and is generally due to 2 differenct causes 1) there is not a strong return form the surface or 2) the planes altitude adjusted quicker than the radar setting and the radar data switches Nyquist Zones. In either case we do not include the data in our dataset. We keep the same number of stacks to keep the same processing scheme and averaging of the radar data for signal to noise consistency. Changed in to from. The Layer indices sentence was rewritten from clarity and figure 3 is cited for a graphic representation.
P6708 L14: Insert "the" before "accumulation rate"	Changed.
P6709 L3-9: Consider moving to the picking section as it seems more appropriate. L16-18: It is not clear which cluster in the crossover analysis show rates off by a factor of two, so perhaps circling it on	We prefer to keep the section on layer numbers detected in result of our procedure. We chose not to add a circle as there are few locations where the factor of 2 is apparent for instance at 0.25 and 0.5. We have changed this figures as suggested later in this reviewers comments so hopefully that will make it clearer. Additionally as shown by the scatter plots these possible errors are not extensive so there are not many

Figure 8 would make it easier.	in the scatterplot. Also shown in the statistics of Table 1.
P6709 L24-26: Consider applying a threshold number of radar measurements for comparison with the MAR grid cell to eliminate comparisons that are likely not as representative.	We keep the comparison as is and not that in all of the grid boxes we have multiple radar-derived measurements. Previous comparisons with ice cores set a precedent that one measurement per grid cell is sufficient. Ie Burgess et al., 2010; Colgan et al., 2015.
P6710 L7-9: The larger differences are associated with areas of higher accumulation. A more informative comparison would be as a percentage. Otherwise, the details in the low accumulation areas are lost. L17-20: The strong statement of "These values are not well correlated: :emphasizing that further improvements in accumulation-rate modeling are needed: : :" should be reworded because the measurements are not without fault, so putting the blame on the model is risky. L27: consider changing "closely" located" to "nearly co-located"	We did not change to percentage difference as we feel the accumulation value is more important for SMB studies. We have change the figures to be clearer as suggested. Reworded to "emphasizing that further improvements in accumulation-rate modeling and measurements are needed, particularly over the southeast and northwest GrIS." Changed.

P6711 L20: consider removing "the" before "large portions" L20-23: Again, this is a very strong statement. It should be changed to state that while these are useful for model evaluation, we must still consider the assumptions that go into the radar-derived measurements. Such a statement would give way for a discussion of the new data needed to reduce those uncertainties.	Removed. We left sentence as "The pattern of radar-derived accumulation rates compares well with known large-scale patterns and clearly shows that these accumulation-rate measurements are useful for evaluating model estimates." As the radar estimates do compare well with large scale patterns and are useful for evaluating model estimates. We address the uncertainties in the radar-derived measurements throughout the paper and again note that our assessment of error is very similar to error assigned by Medley et al. (2013) averaged out to less than 5% (10% and 15% also given) and Das et al. (2015) between 6% and 17% in total SMB.
P6712 L9: consider changing "resolves" to "will resolve" L13: the phrase "constantly varying flightlines" is unclear as to what is varying, please reword	Changed. Changed to " Spatial extrapolation between the flightlines, which vary in position from year-to-year, will be left for future work, as additional data are collected and made available to fill in gaps."
Table 1 Please state in the caption what time interval is used from MAR (July1-April30 or July1-May31). Consider adding a column of the mean accumulation from the crossover points for each year.	Added date clarification. Adding the mean accumulation from the cross over points is likely not a useful number as it is spatially dependent and the crossover are not consistent in space from year to year. We did not add.
General figure comments	The color bar and numbers are held consistent with that

Please change the color intervals used in Figures 4 & 5 to be more meaningful: e.g., 0.2-0.3, 0.6-0.7. The values are non-traditional, making it difficult to quickly interpret the patterns. The black background does not add to the meaning, and is a little ink heavy.	of Burgess et al., 2010 and were not changed. We also choose to keep the Blue Marble as the background image.
Figure 1 Is there overlap between the density measurements (red) and ice core accumulation measurement in blue?	Yes in some locations there are. Added Echogram locations to map.
Figure 2 Please change depths to positive numbers since a depth is positive moving downward. The caption should be very descriptive as to what the differences existing in the timing of the measurements and what model timing is used. This relates to the statements in the beginning on explaining the details of the comparison. For instance,	Added 1 "and the measurements and modeled profiles are contemporaneous." For clarity. Depth changed to positive numbers.

if the average April 30 density profile from MAR is used, please state it. Please do something similar for the measurements as well.	
Figure 3 Please change the Distance values along the x-axis to more appropriate intervals (26, 78, etc. are odd values). An inset map of these transects would be beneficial. They could even be added to Figure 1.	We left the distance values as is and feel they are clearly labeled. The locations of the radagrams were added to figure 1.
Figure 4 Please state that only the accumulation rates from the top layer is plotted for each year in the caption.	Added "representing the top layer in each year (July 1 to April 30). "
Figure 5 Same as with Figure 4, state the time intervals represented here (May1 – April30?). Consider overlaying the radar-derived measurements for comparison	Added" (representing July 1 to April 30 to match the radar-derived estimates)."
Figure 6 The intervals in the legend should be changed to not have overlap: 1, 2-3, 4-6, etc.	Changed.
Figure 7 These values should	Percentages must assume that one pass is more valid

be plotted as percentages rather than absolute values because the crossovers in regions of low accumulation are lost. Also, as described above, the crossover analysis as done here is only a measure of the ability of the picker, so the maps shown here would be better off showing the differences in range bin picks, not in total accumulation. Please be sure to use appropriate intervals for the color bar, if the mean crossover difference was 0.03 m w.e., then majority of them would fall into the first interval.	than the other which we are not able to do. We left figure 7 in m w.e. and changed figure 8 to range bins so the reader is given all of the information. Also change in Table 1.
Figure 8 Similar to Figure 7, this plot should be comparing the picked range bin rather than accumulation rate.	Changed to range bins.
Figure 9 The color bar should be a gradient between two colors, reaching white in the middle in order to appropriately show regions where the model is less than or greater	Changed.

than the measurements. There are too many colors here, making interpretation difficult. Also, be careful with the value intervals making sure the center interval straddles zero evenly (e.g., -0.05-0.05). This way people can easily see the transition between more/less accumulation difference. A histogram of the differences would be a useful addition that can be inlaid onto each map.	
Figure 10 There are a few interesting features here that could be further discussed in the paper. For instance, the 2011 (blue) dots appear to have a linear feature at 0.75x and at 1.5x suggesting the picker detected the 2nd layer rather than the 1st. All the previous plots were broken down by year, it might be useful to do the same (4 plots) to see the details of each as the values <0.5 m w.e. get lost. I would suggest showing the best fit line to the data as well	We do not see in the data that there are mispicks of second layers, there a very few. The differences are likely due to discrepancies between the measurements and the models.

to ease interpretation.	
Figure 11 It would be useful to have the echograms from each year shown as well, so the reader can see the differences in the data between years. It would also lend insight into whether the very large accumulation from the radar in 1995 is due to the picker missing a layer, which is especially interesting because the 2011 data end in 1996.	We did not include the echograms as the data is taken at a single radar trace for this comparison and changed figure 11 as suggested by reviewer #2.

Response to Anonymous Referee#2

First we would like to thank Referee#2 for taking the time to review our paper. We appreciated your comments that have helped to clarify our paper. We will address your comments in the order of the review below.

Response to general comment on mentioning other IceBridge instruments and specifically Accumulation Radar: In Section 3.1 we added the following to address this comment, "Operation IceBridge flights operate multiple instruments, including lidars and radars, spanning a range of frequencies (Koenig et al., 2010; Rodriguez-Morales et al., 2014). The Snow Radar was chosen for this study because the vertical resolution and penetration depth are optimized for our research goal of detecting annual layers from the surface of the ice sheet. It is noted that the CReSIS Accumulation Radar and MCoRDs radars are also capable of detecting accumulation rates on decadal and millennial time scales, respectively, using dated isochrones (e.g. Miège et al., 2013; MacGregor et al., 2015)"

<table>
<tr><th>Specific Comments</th><th>Response</th></tr>
<tr><td>2.1-Modeled density bias below 2.5 m</td><td>We do not see an overestimation bias in the actual data shown in the table below. As you can see the standard deviation is always larger in MAR but the average value is both high and low depending on the depth range. The following sentence is in the paper for clarification, “Below 1 m, the model and observed densities are similar (4% mean difference)”
<table>
<tr><th></th><th>Observed</th><th>MAR</th></tr>
<tr><td>0-1 m</td><td>338 ± 39</td><td>280 ± 40</td></tr>
<tr><td>1 – 15 m</td><td>472 ± 99</td><td>454 ± 158</td></tr>
<tr><td>1 – 2.5 m</td><td>381 ± 54</td><td>387 ± 149</td></tr>
<tr><td>2.5 – 5 m</td><td>436 ± 75</td><td>452 ± 155</td></tr>
<tr><td>5 – 15 m</td><td>531 ± 83</td><td>522 ± 139</td></tr>
</table></td></tr>
<tr><td>2.1- Depth to which analysis was carried out.</td><td>To address this comment we have added a histogram of the depths of the top layer (Figure 7) and added to section 5.1 “Figure 7 shows a histogram of depths for the first layer detected for years 2009 through 2012 where 63% are within the top 1 meter of snow.” We additionally address this more fully in the discussion section.</td></tr>
<tr><td>2.2- Deriving Accumulation from Snow Radar- Standard equation for equation 1 provide more clarity</td><td>We have changed equation 1 into two equations for clarity to show both the accumulation derivation (new equation 1) and the radar travel-time to depth equation</td></tr>
</table>

	(new equation 2) as well as the combined equation (3).. We have also added additional citations to Looyengy, 1965 and Medely et al. 2013, Das et al., 2015 to fully cite these equations. Also added clarification statement on relation of z*rho to cumulative mass in text. Please see section 4.2 in paper for changes as it too extensive to paste here.
2.3 When aligning the surface, outliers in alignment (25 cm out) are discarded. This is fine, but you should state what portion of the data are discarded in this process.	Unfortunately we cannot quantify the amount of data that was discarded due to no surface detection or surface misalignment with our processing chain. We did not keep track of this data and because we also reduce the data size in the process we cannot estimate this based on bytes. We do note that most of these omissions occur when the radar data switched nyquist zones due to airplane altitude adjustments occurring faster than radar adjustments causing the radar data to invert. There is no way to correct this inverted data after the fact and our code was written to just eliminate it from further processing.
2.3 Why stack to 50 meters in one 2011 and 2012, and 10 meters in 2009 and 2010?	Added the following to the paper for clarification in section 4.3.1, “The change in along- track spacing between 2009–2010 and 2011–2012 is due to additional incoherent averaging introduced in 2011. “ We keep the number of stacks equal at 10 but the amount of data released due to the post processing

	change from 2010 to 2011 changes the along track spacing.
2.3-4.3.2 and 4.3.3 sections are not entirely clear. Clarify Spatial and time/depth dimension.	We have attempted to clarify these sections and add description on the along track vs depth/time dimension. Please see sections for changes. We have left only figure 3 for illustration as this is the only graphical output of this process.
2.3-4.3.4 either eliminate or expand.	The authors chose not to eliminate this section as the GUI interface has already been distributed to other researchers and is being use to manually adjust layer for many radar applications for multiple radar systems and needs to be documented. We have expanded as follows," A graphical user interface (GUI) was developed to verify the automated layer detections by displaying the snow-radar radargram and the resulting automated-layer detections. An analyst used the GUI to quickly compare the picked layers and the radargram. The GUI application allows for editing of the output layers as needed including tools for. layers, or parts of layers to be added, deleted, gap-filled, and re-indexed. The GUI saves the analyst time by providing the ability to scroll through all the radargrams and picked layers, including the previous and subsequent along-track data, to detect errors. Statistics on the error rates of the automatic algorithm were not keep,

	however, it is noted that the error rates depend on the quality of the radar data, influenced by both radar and aircraft operations, and the regional characteristics of the firn microstructure which can either preserve or erode layering. “
2.4 Results- Why not normalize to 12 months.	Intentionally we do not want to normalize to 1 year. When comparing to modeled data we can compare on a monthly (or daily) basis. The Snow Radar performance is best on identifying the top layer, a partial year, and we compare it to modeled data from the same time. We do spend a full paragraph describing this because it does need to be documented for comparison with other data, like ice cores, in which case you would likely want to normalize to a year. We do not make this assumption since the modeled data is run over the same period for accumulation.
2.4 Figure 5	We prefer to keep figure 5 as it shows the year to year variability in the model as well as differences in spatial patterns between MAR and snow radar maps such as the lack of the higher accumulation region in Northeast Greenland in the MAR maps which is seen in snow radar and discussed in the paper.
2.4 Section 5.2 Interpolation of MAR, Year 2010 comment	Because MAR is generating accumulation based on topography we do not feel it is appropriate to downscale the model.

	Theoretically the radar should be sampling the accumulation variability across the MAR grid cell and the average would be simulated by MAR, hence, we have averaged all samples within a MAR grid cell for this comparison. This is similar to techniques used by Medley et al., 2013 in a similar study in Antarctica. Yes 2010 is a particularly difficult year. This could be do to a few reasons 1) MAR did not do well that season 2) the snow radar data is more limited in spatial extent and is sampling preferentially in the North and Southeast where MAR seems to have more trouble even in other years. It always must be kept in mind that airborne data is not a systematic spatial sampling and in years that the aircraft targeted different geographic regions the model may look worse but it is a spatial sampling bias due to the aircraft data. 2010 is likely a combination of both of these effects.
2.4-Page 6731 Figure 11- Illustrate as step plots	We have changed the figure a step plot to accurately represent the dates over which the accumulation is average. Your final comment in this section in reference to Camp Century, "you should report you 11will actually probably make your result look in better agreement.." is unclear and likely a typo. Please let us know what this comment

	was aimed at so we can address.
2.4 Single 2001 date	Yes there is an explanation for this and that is the 2001 and 2002 layers were dated from the surface in the interior of the ice sheet along the flight line going into Camp Century. The 2001.5 and 2002.5 layers were strong reflectors and were traced continuously to Camp Century. The layers above were not as strong and were not traced over that distance. This doesn't occur very often in our dataset but there are a few layers at depth, particularly in Northern Greenland, that are continuously traced and dated from the interior. In short this data comes from a traced layer date, not from the surface at the exact location of Camp Century.
Technical Corrections	**Response**
Page 6699, lines 21-24: This sentence is awkward and not entirely clear. Clarify	Change to "As GrIS mass loss has accelerated, a fundamental change the mass loss process has occurred. The dominant mass loss process for the GrIS has changed from being dominated by ice dynamics to being dominated by surface mass balance (SMB) processes, which include accumulation and runoff (van den Broeke, 2009; Enderlin et al., 2014)."
Page 7600, line 3: "here after" should be "hereafter"	Corrected.
Page 7601, line 6: "to monitor decadal-	Changed.

scale..." monitor is not really appropriate here- change to "measure"	
Page 7601, line 6: "to monitor decadal-scale..." monitor is not really appropriate here- change to "measure"	Changed.
Page 7601, line 27: GCM is more frequently a "General Circulation Model" as opposed to "Global Climate Model". However, since you only are using RCMs here, why not just eliminate the mention of GCM?	Changed to General Circulation Model as they too can provide spatially and temporally extensive estimates of accumulation-rate fields at ice-sheet scales
Page 6703, line 25: "an additionally" should be "an additional"	Changed.
Page 6704, line 5: this sentence is awkward- the phrase "that cover and vary" in particular is kind of confusing. Suggest just removing "and vary" since the statement that there are multiple profiles implies variability.	Removed.
Page 6704, line 6: "from the MAR model" is redundant- just use "from MAR" which is what you use elsewhere.	Changed.
Page 6706, line 4-6" The sentence "Equation (1) is written to show the relationship between the density profile, which is used for ... This is not a "between" situation, as	Changed to "Equation 1 is written to show that the density profile is used both for calculating depth and water equivalent"

we’re talking about one thing. I suspect this is a copy/paste error.	
Page 6706, line 16: No need to mention the Onana et al layer picker, as you don’t use it! Remove this sentence.	Removed.
Page 6706, line 13 and throughout: Active voice is much easier to read than passive voice, though this is a style thing and should be left to the discretion of the editor.	Changed.
Page 6707, line 1: "minimize data noise" eliminate ’data’ from this, not a useful word here. It’s all data...	Removed.
Page 6711, line 4: "whereas as the" delete ’as’.	Removed.
Page 6712, line 24: "filled to broaden with" delete ’to broaden’	Removed
Page 6726, Caption to figure 6: English usage- "less than three layers" should be "fewer than three layers" since we cannot have a fraction of a layer.	Changed.

Annual Greenland accumulation rates (2009-2012) from airborne Snow Radar

L.S. Koenig[1], A. Ivanoff[2], P.M. Alexander [3,4], J. A. MacGregor[4~~5~~], X. Fettweis[5~~6~~], B. Panzer[6~~7~~], J.D. Paden[6~~7~~], R.R. Forster[7~~8~~], I. Das[8~~9~~], J. McConnell[9~~10~~], M. Tedesco[3~~4~~,9], C. Leuschen[6~~7~~] and P. Gogineni[6~~7~~]

[1]{National Snow and Ice Data Center, University of Colorado, Boulder, CO, USA}

[2]{ADNET Systems, Inc., Bethesda, MD, USA}

[3]{NASA Goddard Institute for Space Studies, New York, NY, USA}

~~[4]{City College of New York, New York, NY, USA}~~

[~~[~~4~~5~~]{Cryospheric Sciences Laboratory (Code 615), NASA Goddard Space Flight Center, Greenbelt, MD~~Institute for Geophysics, The University of Texas at Austin, Austin, TX~~, USA}

[5~~6~~]{Department of Geography, University of Liège, Belgium}

[6~~7~~]{Center for Remote Sensing of Ice Sheets, University of Kansas, Lawrence, KS, USA}

[7~~8~~]{Department of Geography, University of Utah, Salt Lake City, UT, USA}

[8~~9~~]{Lamont-Doherty Earth Observatory, Columbia University, New York, NY, USA}

[9~~10~~]{Division of Hydrologic Science, Desert Research Institute, NV, USA}

Correspondence to: L.S. Koenig (lora.koenig@colorado.edu)

Abstract

Contemporary climate warming over the Arctic is accelerating mass loss from the Greenland Ice Sheet ~~(GrIS)~~ through increasing surface melt, emphasizing the need to closely monitor its surface mass balance ~~(SMB)~~ in order to improve sea-level rise predictions.~~-~~ Snow accumulation is the largest component of the ice sheet's surface mass balance, but in situ observations thereof are inherently sparse and models are difficult to evaluate at large scales. Here, we quantify recent Greenland accumulation rates~~, the largest component of GrIS SMB, at a higher spatial resolution than currently available, using~~ using ultra-wideband (2–6.5 GHz) airborne Snow Radar data collected as part of NASA's Operation IceBridge between 2009 and 2012~~Snow Radar stratigraphy~~. We use a semi-automated method to ~~derive~~ trace the observed radiostratigraphy and then derive annual-net accumulation rates ~~from airborne Snow Radar data collected by NASA's Operation IceBridge from~~ for 2009 to 2012. The uncertainty in these radar-derived accumulation rates is up to 12%, attributed mostly to uncertainty in the snow/firn density profile. A comparison of the radar-derived accumulation rates and

contemporaneous ice cores shows that Snow Radar captures both the annual and long-term mean accumulation rate accurately. ~~An initial~~ A comparison ~~of the accumulation rates from the Snow Radar and the~~ with outputs from ~~of~~ a regional climate model (MAR) shows that, ~~in general, the~~this model matches radar-derived accumulation ~~matches closely with MAR~~ rates in the ice sheet interior ~~of the ice sheet~~ but ~~MAR c~~overestimates ~~are high~~ over ~~the~~ southeastern Greenland~~rIS~~. ~~Comparing the radar-derived accumulation with contemporaneous ice cores reveals that the radar captures the annual and long-term mean. The radar-derived accumulation rates resolve large-scale patterns across the GrIS with uncertainties of up to 11%, attributed mostly to uncertainty in the snow/firn density profile.~~Our results demonstrate that Snow Radar can efficiently and accurately map patterns of snow accumulation across an ice sheet, and that it is valuable for evaluating the accuracy of surface mass balance models.

1 Introduction

Contemporary climate warming over the Greenland Ice Sheet (GrIS) has accelerated its mass loss, nearly quadrupling from ~55 Gt a^{-1} between 1993-99 (Krabill et al. 2004) to ~210 Gt a^{-1} ~~of ice~~, equivalent to ~0.6 mm a^{-1} of sea level rise, between 2003-08 (Shepherd et al. 2012). As GrIS mass loss has accelerated, a fundamental change in the ~~nature of this~~ dominate mass loss process has occurred (e.g. Tedesco et al., 2015). ~~The dominant mass loss process for the GrIS is~~It switched from ~~changing from being governed by~~ ice dynamics to ~~being dominated by~~ surface mass balance (SMB) processes, which include accumulation and runoff (van den Broeke, 2009; Enderlin et al., 2014). This recent shift emphasizes the need to monitor SMB which, over most of the GrIS, is dominated by net accumulation.

Here, we use the complete set of airborne Snow Radar data collected by NASA's Operation IceBridge (OIB) over the GrIS from 2009 to 2012 to produce net-annual ~~net~~ accumulation rates, here~~-~~after called accumulation rates for simplicity, along those flightlines. The radar-derived accumulation rates are compared to both in situ data and model outputs from the Modèle Atmosphérique Régional (MAR).

2 Background

In situ accumulation-rate measurements are limited in number by the time and cost of acquiring ice cores, digging snow pits or monitoring stake measurements across large sectors of the ice sheet. Only two major accumulation-rate measurement campaigns have been undertaken across the GrIS.~~,~~ T~~t~~he first in the 1950's when the US Army collected pit data along long traverse routes (Benson, 1962), and the second in the 1990's when the Program on

Arctic and Regional Climate Assessment (PARCA) collected an extensively distributed set of ice cores (e.g. Mosley-Thompson et al., 2001). A recent traverse and study by Hawley et al. (2014) reports a 10% increase in accumulation rate since the 1950's and highlights the need to monitor how Greenland precipitation is evolving in the midst of ongoing climate change. Although many other accumulation-rate measurements exist, they are more limited in either space or time (e.g. Dibb and Fahnestock, 2004; Hawley et al. 2014).

To date there is no annually resolved satellite-retrieval algorithm for accumulation rate across ice sheets. Hence, the two primary methods used to generate large-scale (hundreds of km) accumulation-rate patterns are model predictions and radar-derived accumulation rates (Koenig et al., 2015). High resolution, near-surface radar data have shown good fidelity at mapping spatial patterns of accumulation over ice sheets at decadal and annual resolutions from both airborne and ground-based radars (Kanagaratnam et al., 2001; 2004; Spikes et al., 2004; Arcone et al., 2005; Anshütz et al., 2008; Müller et al., 2010; Medley et al., 2013; Hawley et al., 2006; 2014; de la Peña et al., 2010; Miège et al., 2013). Radars detect ~~and map~~the lateral persistence of isochronal layers within the firn. When these layers are either 1) dated in conjunction with ice cores or 2) annually resolved from the surface, they can be used to determine along-track accumulation rates.

Early studies by Spikes et al. (2004) in Antarctica and Kanagaratnam et al., (2001 and 2004) in Greenland used high/very high-frequency (100 to 1000 MHz) ground-based and airborne radars, with vertical resolutions of ~30 cm, to ~~monitor~~ measure decadal-scale accumulation rates between dated ice cores. These high/very high-frequency radars can penetrate ~~to~~ hundreds of meters in the dry-snow zone and tens of meters in the ablation zone (Kanagaratnam et al., 2004). Subsequent studies utilized the larger bandwidths of ultra/super-high frequency (2 to 20 GHz), frequency-modulated, continuous wave (FMCW) radars~~,~~ with centimeter-scale vertical resolutions capable of mapping annual layers within ice sheets (e.g. Legarsky 1999; Marshall and Koh, 2008; Medley et al., 2013). Ultra/super-high frequency radars can penetrate tens of meters in the dry-snow zone and meters in the ablation zone. Legarsky (1999) was among the first to show that such radars could image annual layers, and Hawley et al. (2006) further demonstrated that a 13.2 GHz (Ku-band) airborne radar imaged annual layers in the dry-snow zone of the GrIS to depths of up to 12 m.

Most previous studies used radar data that overlapped spatially with ice cores or snow pits for both dating layers and density information. Medley et al., (2013) and Das et al.

(2015~~), however,~~) showed that accumulation rates could also be derived using density from a regional ice core ensemble. The end members of density are used as the uncertainty limits and the derived regional density profile is sufficient for radar studies of accumulation and SMB (Das et al, 2015). Additionally, Medley et al. (2013) showed that the Snow Radar was capable of resolving annual layering in high accumulation regions where the layers were preserved; ~~and,~~ therefore, it was possible to date the layers by counting from the surface downwards.

Regional Climate Models,~~ and~~ General ~~Global Climate~~ Circulation Models (RCMs and GCMs) and reanalysis products provide the only spatially and temporally extensive estimates of accumulation-rate fields at ice-sheet scales (e.g. Burgess et al., 2010; Hanna et al., 2011; Ettema et al., 2009; Fettweis, 2007; Cullather et al., 2014). In a comprehensive model intercomparison study, Vernon et al. (2013) found that modelled accumulation rates had the least spread across the RCM's considered, but still had a ~20% variance. Chen et al. (2011) found the range in ~~average~~ mean accumulation rate across the GrIS between five~~5~~ reanalysis models to be ~15 to 30 cm a^{-1}~~/yr~~, while Cullather and Bosilovich (2011) found the range in ~~average~~ mean accumulation rate across the GrIS between reanalysis data and RCM's to be ~34 to 42 cm a^{-1}~~/yr~~. ~~Overall, while~~While these models continue to improve, there is clearly a continuing need for large-scale accumulation-rate measurements to evaluate their outputs.

3 Data, instruments and model description

3.1 Snow radar and data

Annual layers in the GrIS snow/firn were mapped using the University of Kansas' Center for Remote Sensing of Ice Sheets (CReSIS) ultra-wideband Snow Radar during ~~NASA's Operation IceBridge (~~OIB~~)~~ Arctic Campaigns from 2009 through 2012 (Leuschen, 2014). The Snow R~~r~~adar operates over the frequency range from ~2 to 6.5 GHz (Panzer et al., 2013; Rodriguez-Morales et al., 2014). The Snow Radar uses an ~~a Frequency Modulated Continuous Wave (~~FMCW~~)~~ design to provide a vertical-range resolution of ~4 cm in snow/firn, capable of resolving annual layering, where~~n~~ preserved, to tens of meters in depth (Medley et al., 2013). OIB flights operate multiple instruments, including lidars and radars, spanning a range of frequencies (Koenig et al., 2010; Rodriguez-Morales et al., 2014). The Snow Radar was chosen for this study because its vertical resolution and penetration depth is

Formatted: Superscript

optimized for detecting annual layers from the surface of the ice sheet. It is noted, however, that the CReSIS Accumulation Radar and MCoRDs radar are also capable of detecting accumulation on decadal to multi-millennial time scales, respectively, using dated isochrones (e.g. Miège et al., 2013; MacGregor et al., 2016)

3.2 Modelled accumulation rates and density

Accumulation rate and snow/firn density profiles were derived from the MAR RCM (v3.5.2; X. Fettweis, pers. comm., 2015). MAR is a coupled surface-atmosphere model that simulates fluxes of mass and energy in the atmosphere and between the atmosphere and the surface in three dimensions, and is forced at the lateral boundaries with climate reanalysis outputs (Gallée, 1997; Gallée and Schayes, 1994; Lefebre et al., 2003). It incorporates the atmospheric model of Gallée and Schayes (1994), and the Soil Ice Snow Vegetation Atmosphere Transfer scheme (SISVAT) land surface model, which includes the multi-layer Crocus snow model of Brun et al. (1992). The MAR v3.5.2 simulation used here utilizes ~~reanalysis~~ outputs from the European Center for Medium Range Weather Forecasting (ECMWF) ERA-Interim global atmospheric reanalysis (Dee et al., 2011) at the lateral boundaries, with a horizontal resolution of 25 km. ~~The~~Additional details ~~of this setup~~ are described ~~further~~ by Fettweis (2007), with ~~further~~ updates described by Fettweis et al. (2011; 2013) and Alexander et al. (2014). MAR has been validated with in situ data and remote sensing data over the GrIS, including data from weather stations (e.g. Lefebre et al., 2003; Fettweis et al., 2011), in situ and remot~~e~~ely sens~~ing~~ed albedo data (Alexander et al., 2014), and ice-core accumulation-rates ~~estimates~~ (Colgan et al., 2015), and it has been used to model both past and future SMB (Fettweis et al., 2005; 2013). We use accumulation ~~-~~rates and density profiles simulated by MAR for the period during which the radar data were collected (2009 to 2012).

In MAR, the initial falling snow density ($\rho_{s,0}$) is parameterized as a function of surface air temperature (T_{air}) in °C and windspeed (V) in m s^{-1} as

$$\rho_{s,0} = \max(30, 109 + 6T_{air} + 26\sqrt{V}.$$

After falling to the surface, snow densification in MAR is described according to the scheme of Brun et al. (1989) where the densification rate (dz/dt) at depth (z) is

$$\frac{dt}{dz} = \frac{-\sigma z}{C\rho} 250 e^{(-0.023\rho + 0.1|T|)},$$

Formatted: Superscript

Formatted: Centered

Formatted: Centered

where ρ is density (kg m^{-3}) and T temperature (°C) at depth z (m), σ is the vertical stress from the snow above (kg $m^{-1}s^{-1}$) and C is a function of snow grain size and snowpack liquid water content.

3.3 In situ density and accumulation-rate data

The SUrface Mass balance and snow depth on sea ice working groupup (SUMup) dataset (July 2015 release) contains a compilation ofcompiles publically available accumulation-rate, snow depth and density measurements over both sea ice and ice sheets (Koenig et al., 2012). We use two subsets of theseis data. First, to characterize density across the GrIS, we extract the snow/firn density measurements ranging in depth from the snow surface to 15 m (the depth to which MAR predicts firn densityies), which contains over 1500 measurements from snow pits and ice cores at 62 sites. At each site, the number of measurements ranges in number between 8 and 170 and maximum depths range from 1 to 15 m. (Koenig et al., 2015; Koenig et al., 2014; Miège et al., 2013; Mosley-Thompson et al., 2001; Hawley et al., 2014; Baker 2015) (Figure 1). Second, to compare radar-derived and measured in situ accumulation rates, we consider only accumulation-rate measurements within 5 km of OIB Snow Radar data, a criterion that includes 11 ice cores from the SUMup dataset (Mosley-Thompson et al., 2001). To expand this comparison, an additionally dataset of 71 ice cores (J. McConnell, pers. comm., 2015) which includes additional cores to the SUMup dataset, was included, used to locate accumulation measurements within 5 km of OIB Snow Radar data providing 23 additional ice cores within 5 km of OIB Snow Radar data (Figure 1).

4 Methods

4.1 Determining the density profile and uncertainties

Because we seek to derive accumulation rates from near-surface radars across large portions of the ice sheet, we require firn density profiles that cover and vary across the entire GrIS. Modelled snow/firn density profiles from the MAR model were investigated for use. However, a preliminary comparison of the SUMup-measured density profiles to MAR-estimated density profiles showed that MAR– simulated density values in the top 1 m of snow/firn were significantly lower (0.28004 ± 0.0450 g cm^{-3}) than observed (0.338 ± 0.039 g cm^{-3}) (Figure 2). The comparison of measured and modeled density was simultaneous in time, meaning that the MAR density profile output on the day of the measurement was used in this comparison. We consider it beyond the scope of this study to investigate and explain why MAR underestimates near-surface density, therefore, here we assume that the firn density in the top 1 m is 0.338 g cm^{-3}. Below 1 m, the model and observed densities are similar (4% mean difference with the model generally overestimating measured density slightly), so the spatially-varying modelled density profiles are used for April 30 of each year. Hence, a hybrid measured-modelled density profile is used to determine accumulation rates from the snow radar data (Figure 2).

Uncertainty in the top meter is assigned by the ±1σ variation in observed density (12%) which we assume is due to the natural variability in surface density. We note that this uncertainty is broadly consistent with that which we expect due to natural variability in surface density across the GrIS. This natural variation, however, represents a smaller assumed error uncertainty than the mean difference between the modelled and observed values within the top 1 m (16%).

4.2 Deriving accumulation rates from Snow Radar and uncertainties

The radar travel time is converted to depth (z) using the snow/firn density profile and the dielectric mixing model of Looyenga (1965). Possible Eerrors in radar-derived depth come from two primary sources: 1) the dielectric mixing model chosen and 2) layer picking. The choice of the dielectric mixing model maximizes potential error at a density of ~0.300 g cm^{-3}. The maximum possible difference in depth over 15 m is 3% assuming a constant density of 0.320 g cm^{-3} and <1% assuming a constant density of 0.600 g cm^{-3} (Wiesmann and Matzler, 1999; Gubler and Hiller, 1984; Schneebeli et al., 1998; Looyenga, 1965; Tiuri et al., 1984). The second source of error occurs during manual adjustment of the picked layers (Section 4.3.4) and is estimated to be ±3 range bins, or ~8 cm.

The Aaccumulation rate at along-track location rate is derived using the standard equation for converting depth from a radar profile to accumulation rates at location (x is derived by):

$$\dot{b}(x) = \frac{z\,TWT(x)\rho(x)\epsilon}{2a(x)\rho_w\left(\frac{\rho(x)}{\rho_i}\left(\varepsilon'_i{}^{1/3}-1\right)+1\right)^{3/2}} \quad (1)$$

Formatted: Font: Times New Roman

Where $\dot{b}$ is water equivalent accumulation rate in m w.e. a^{-1}, z is the depth of layer in m*TWT* is the two-way travel time to the date layer in sec, ρ is cumulated snow/firn density to at that depth z in kg m^{-3}., Hence, the numerator the cumulative mass in kg m^{-2} to depth z *c* is the speed of light in m s^{-3}, *a* is age of the layer in years from the date of radar data collection and ρ_w is the density of water in kg m^{-3} (e.g. Medely et al., 2013; Das et al., 2015). Depth z is calculated using the radar two-way travel time (*TWT*), the snow/firn density (ρ) and the Looyenga (1965) dielectric mixing relationship as follows:

$$z = \frac{TWTc}{2\left(\frac{\rho}{\rho_i}\left({\varepsilon'_i}^{1/3}-1\right)+1\right)^{3/2}}. \qquad (2)$$

Where *TWT* is the travel time to the dated layer in sec, *c* is the speed of light in m s^{-3}, ρ_i is ice density in kg m^{-3} and ε'_i is the dielectric permittivity of pure ice. Combining these two equations gives:

$$\dot{b}(x) = \frac{TWT(x)\rho(x)c}{2a(x)\rho_w\left(\frac{\rho(x)}{\rho_i}\left({\varepsilon'_i}^{1/3}-1\right)+1\right)^{3/2}}. \qquad (3)$$

The cumulative mean snow/firn density (ρ) is determined by the density profile previously described in Section 4.1. The layers are picked in the radar data using a semi-automated approach described in (Section 4.3).

Layer ages are determined by assuming spatially continuous layers are annually resolved and dated accordingly from the year the radar data were collected. The radar data were collected during springtime (April-May) and the surface is assumed to be 30 April. The picked layers at depth are assumed to be 1 July ±1 month as follows, therefore, the first layer represents 10 months and each subsequent layer is 12 months. PA peaks in radar reflectivity areon, assuming ice with no impurities, is caused by the largest change in snow density. In the ablation and percolation zone, the peak in density difference occurs in the summer between the snow layer and ice or the snow/firn layer and the high-density melt/crust layer, respectively (e.g. Nghiem et al., 2005). In the dry snow zone, thee peak in density difference contrast also occurs in the summer between the summer hoar layer and the denser snow/firn layer (e.g. Alley et al., 1990). While melt/crust and hoar layers can form at other times, it is assumed they will be smaller and, therefore, cause a smaller radar reflection than the dominate layers which occur near 1 July.

Formatted: Font: Italic

Formatted: Font: Italic

Formatted: Centered

Formatted: Font: Italic

Formatted: Centered

To calculate the total uncertainty on the radar-derived accumulation rate, the maximum error is assumed for both density (12%) and age (10~~8~~%, in the first layer and 8% in subsequent layers). Equation ~~1~~ 3 ~~is written to~~ shows that the ~~relationship between the~~ density profile~~, which~~ is used ~~both~~ for calculating both depth and water equivalent. The derivative of Equation 3~~1~~ ~~is used to~~ determines the correlated error between depth and density. Assuming uncorrelated and normally distributed errors between density and age, the maximum accumulation-rate uncertainty is 12~~1~~%, with uncertainty in the density profile in the top meter of firn being the largest contributor. This relative u~~U~~ncertainty ~~from our study~~ is ~~very~~ similar to previous studies by Medley et al. (2013) and Das et al. (2015) for radar-derived accumulation rates.

4.3 Semi-Automated Radar Layer Picker

A semi-automated layer detection algorithm ~~was~~ is developed to process the large amounts of OIB Snow R~~r~~adar data ~~gathered by OIB~~ (>10^4 km $year^{-1}$), analogous to the challenges faced by MacGregor et al. (2015) for analysis of very high frequency ~~"deep"~~ radar sounder data. ~~A previously developed semi-automated method designed by Onana et al. (2014) was tested for this application but proved too computationally intensive, with higher error rates than the method described here.~~ While a fully automated method is ultimately desirable, we have found that it is necessary to manually check every automated pick, making adjustments as needed by an experienced analyst, to distinguish between spatially discontinuous radar reflections~~ors~~, caused by the ~~norma~~natural heterogeneity of firn microstructure, and spatially consistent annual layers. ~~The~~ Our algorithm processes the OIB Snow Radar data in four steps outlined below.

4.3.1 Surface Alignment

~~4.3.2~~ The snow surface is detected by a threshold, set to four times the mean radar return from air, which is assumed to be the radar background noise level. A median filter is applied vertically to each radar trace to minimize ~~data~~ noise. ~~In addition, any~~Any surface detection~~value~~ that is displaced by greater than~~exceeds a distance threshold of~~ 10 range bins (~25 cm) from ~~its neighbors~~its adjacent traces is not used and that entire vertical trace is ignored in subsequent analysis. Data arrays are then aligned to the surface and truncated above and below the surface (200 and 800

Formatted: Indent: First line: 0.25", No bullets or numbering range bins, respectively), equivalent to ~25 m into the snow/firn, to reduce data volumes. Layer depths are measured relative to the snow surface. The radar data are then horizontally averaged (stacked) 10 times to an along-track spacing of ~~~50 m, in 2011 and 2012, and~~ ~10 m~~, in~~ (2009 and 2010) and ~50 m (2011 and 2012), and split into equally sized sections of 2000 traces per radargram for easier processing. The change in along-track spacing between 2009–2010 and 2011–2012 is due to additional incoherent averaging introduced in 2011.

Formatted: Indent: First line: 0"

~~4.3.3~~ 4.3.2 Layer Detection

Formatted: Indent: First line: 0.25", No bullets or numbering

The algorithm takes advantage of the difference between high-frequency and low-frequency spatial variability in the traveltime/depth domain to identify peaks in returned power in the radar data. Such p~~P~~eaks are formed by the stratified accumulation layers of interest in this study, and they~~, resulting in density changes, which extend across the GrIS. The point at which the peak~~ form~~s~~ ~~occurs~~ over ~~a~~ small spatial scale~~s~~s, ~~or at a~~ equivalent to high frequency, in the traveltime/depth domain. ~~The~~ Our peak detection process is thus a type of high-pass filter, resulting in the set of disjointed points detected at radar reflection peaks in the time domain and in adjacent traces along the flight path. These points are ~~are stored~~connected into~~as~~ continuous layer segments using the half-maximum width of ~~the~~ each peak's waveform~~, resulting in continuous layer segments over the radar data profile~~ (Figure 3, locations of radargrams shown in Figure 1).

~~4.3.4~~4.3.3 Layer indexing

Formatted: Outline numbered + Level: 3 + Numbering Style: 1, 2, 3, … + Start at: 1 + Alignment: Left + Aligned at: 0.25" + Tab after: 0.75" + Indent at: 0.75"

Each along-track detected layer is indexed, with both a number and the corresponding year, counting down from the surface detection (Figure 3). ~~This process is accomplished by indexing the layers downward from the surface.~~ This~~e~~ indexing ~~process~~ begins with the segmentation of the layers, so that each layer is uniquely ~~identifi~~identified with a layer number~~iable~~. The peak points within each segment are ~~then~~ connected by ~~smoothed~~ spline fittings~~s~~, resulting in a set of sharply defined along-track layers at different depths (Figure 3). These layers represent 1 July in the appropriate year counting from the surface and the year collected. ~~Layer indices are assigned from top to bottom to take into account the partial overlap that can exist between layers.~~

4.3.54.3.4Manual adjustment with the Layer Editor

A graphical user interface (GUI) was developed to verify the automated layer detections by displaying the Snow-Radar radargram and the resulting automated-layer detections. An analyst usesd the GUI to quickly visually compare the picked layers and the radargram. The GUI application allows for layer editing of the output layers as needed including tools for. layers, or parts of layers to be added, deleted, gap-filled, and re-indexed. The GUI accelerates layer picking by providing the ability to scroll through all the radargrams and picked layers, including the previous and subsequent along-track data, to detect errors. Scrolling allows for spatially continuous layers, which may not be datable at all locations, to be propagated and dated from a location where annually resolved layers are evident from the surface. Error statistics for the automatic algorithm were not kept, but depend generally on the quality of the radar data, influenced by both radar and aircraft operations, and the regional characteristics of the snow/firn microstructure, which can either preserve or erode layering.

5 Results

5.1 Radar-derived accumulation rates over the GrIS

Annual radar-derived accumulation rates and their uncertainties were calculated for all 2009–2012 OIB radar data that contained detected layers (Figure 4). The increase in coverage from 2009 to 2012 is related to an increasing number of OIB flights over the GrIS and adjustments to the Snow Radar antenna and operations that improved overall data quality. These accumulation-rate patterns are consistent with observed and modelled large-scale spatial patterns for the GrIS: high accumulation rates in the southeast-coastal sector and lower accumulation rates in the northeast (Figure 5). Year-to-year variability in the accumulation rate is also evident,t and can be seen even at the ice-sheet scale, e.g., in the southeast accumulation rates were lower in 2010 than in 2011.

The radar-derived accumulation rate in Figure 4 represents only the first layer detected by the Snow Radar, or approximately the annual accumulation rate from the year prior to data collection. For simplicity, we refer to this quantity as the annual accumulation rate, but we caution that it does not strictly represent the calendar year. The values shown in Figure 4 represent only 10 months of accumulation, based on our assumption that the radar layers date to 1 July (Section 4.2) and that the data collection date is 30 April for all OIB data. When comparing the first layer of radar-derived accumulation to modelled estimates from MAR

(Figure 5) or other accumulation measurements, this timing difference must be considered. Although the first layer represents only a partial year, all deeper layers represent a full year, from 1 July to 30 June. We simultaneously compare the time represented by the layer to MAR estimates of accumulation.

Figure 6 shows the number of detected layers, or previous years, discernable in the OIB radar data. For the majority of the GrIS, 1 to 3 annual layers are discerna~~a~~ble~~, due to the spatial distribution of OIB flightlines~~. OIB flightlines are clustered in the ablation/percolation zones of the GrIS, where radar penetration depths are reduced by the increased density, englacial water and layering structure of the firn column (Figure 3). In the GrIS interior, where dry snow conditions allow deeper radar penetration, annual layering going back over two decades is detectable (Figure 3). Figure 7 shows a histogram of depths for the first layer detected for years 2009 through 2012; 63% are within the top 1 meter of snow.

Crossover points were assessed to determine the internal consistency of the radar-derived accumulation rates (Figure 8~~7~~ and~~and Figure~~ 9~~8~~). While no consistent spatial pattern is found in the crossover errors, the largest discrepancies were found in 2011 and 2012 in the northwest and southeast (Figure 8~~7~~). Other inconsistencies are likely due to snow storms occurring between flights in the southeast and incorrectly picked layers that were either sub- or multi-annual in the northwest. Figure 9~~8~~ shows a scatterplot of crossover points. There are relatively few outliers, and those that are outlying are generally offset by a factor of two, suggesting an error in layer detection/dating rather than a radar-system error. Crossover differences per year, including the mean, standard deviation and maximum, are ~~listed~~ given in Table 1. ~~Crossover~~ These differences are comparable (mean of 0.04 m w.e. a^{-1} or 4 range bins) to our inferred relative uncertainty of 12~~1~~% which emphasizes the overall validity of our chosen methods.

5.2 Comparison with modelled accumulation

The radar-derived accumulation rate was gridded to the MAR grid for comparison. The mean-local, radar-derived accumulation rate was used when gridding. Because OIB flightlines are not spatially heterogeneous, each MAR grid cell represents a different number of radar-derived values, so grid cells are not sampled equally. With this discrepancy noted, this gridding method is still the most straightforward ~~and useful~~ approach for this comparison. Figure 10~~9~~ shows the difference between the radar-derived and MAR accumulation rates.

The mean difference for all years is low (0.02 m w.e. a^{-1}). Table 1 shows the annual variability of the mean difference, which is low for every year except 2010, when large differences are seen over the southeast coastal region of the GrIS (Figure 10~~9~~).

Figure 10~~9~~ shows that MAR generally predicts accumulation rates well in the GrIS interior (consistent with the comparison with ice core estimates presented by Colgan et al., (2015)), but has larger errors around the periphery, especially in the southeast and northwest. In the southeast, MAR generally overestimates accumulation rates, except in 2011 when there is a mixed pattern of agreement and overestimation. This pattern of overestimation in the southeast is not surprising and is likely due to the lack of previous measurements in the region to constrain accumulation rates and the large changes in surface topography that are not resolved by the relatively large grid size used in modelled estimates (Burgess et al., 2010). In 2011, the northwest coastal region of the GrIS was well sampled by OIB and MAR ~~shows an~~ underestimat~~esion of~~es accumulation rates there. The~~, but the~~ origin of this anomaly is less clear, but may be related to forcing at the lateral boundaries of MAR that does not capture a relatively small storm track into this region.

Figure 10 shows a scatterplot of the radar-derived and MAR-estimated accumulation rates. These values are not well correlated (Pearson correlation coefficient r^2 = 0.2) and have large RMSE (0.24 m. w.e. a^{-1}), emphasizing that further improvements in accumulation-rate modeling and measurements are needed, particularly over the southeast and northwest GrIS.

5.3 Comparison with annually resolved in situ data

Between 2009 and 2012, OIB flew within 5 km of 34 ~~ice~~ core locations but only two locations, NEEM and Camp Century (Figure 1) were coincident in time with the layers we detected. Each of these locations has two cores, providing annual accumulation rates and a measure of spatial variability. Figure 12~~1~~ compares the radar-derived to ~~ice~~ core measured accumulation rates. At NEEM, the two ice cores and radar data are ~~closely~~ nearly co-located, within 0.6 km of each other. The radar-derived accumulation rates are self-consistent between 2011 and 2012 and agree well with the ice cores (r~~R~~oot m~~M~~ean s~~S~~quare e~~E~~rror (RMSE) of 0.06 m w.e. a^{-1}). For comparison, the two NEEM ~~ice~~ cores have a RMSE of 0.05 m w.e. a^{-1} for the period of overlap. A timing discrepancy arises with this comparison because the ice cores, with higher dating resolution from isotopic and chemical analysis, are dated and reported as the calendar year, whereas ~~as~~ the radar-derived accumulation is assumed 30 June - 1 July (Section 4.2). This mismatch in the measurement is likely evident in Figure 12~~1~~ by the differences in the annual peaks between the cores and radar-derived accumulation having similar means yet differing magnitudes from year to year.

Near Camp Century, the ~~ice~~ cores and radar data are farther apart from each other. The radar-data are located within 4.4 km of the Camp Century core and the GITS core is located ~8.2 km from the Camp Century core. These separations are likely responsible for the poorer agreement at this site of radar-derived accumulation rate to the Camp Century core (RMSE 0.10 m w.e. a^{-1}) and the larger difference (RMSE 0.07 m w.e. a^{-1}) in accumulation rate between the two cores for the period of overlap. At Camp Century, and throughout much of northern Greenland, two older, continuous layers were dated from the interior of the ice sheet and spatially traced. These layers, dated 2000.5 and 2001.5, could not be dated with the Camp Century data alone and, hence, the temporal gaps in annual accumulation at this location. While it is more difficult to analyze the results at Camp Century, with only three~~3~~ points of overlap and no continuous annual time series of radar-derived accumulation rates, ~~it is evident that the radar-derived accumulation rates~~our estimates are within the expected variability and capture the long-term mean value.

6 Discussion

This study is the first to derive annual accumulation rates from near-surface airborne radar data collected across ~~the~~ large portions of the GrIS. The pattern of radar-derived accumulation rates compares well with known large-scale patterns and clearly shows that these accumulation-rate measurements are useful for evaluating model estimates. At the two locations with contemporaneous cores, ~~the~~ radar-derived rates agree well with the long-term mean. Additional cores, with direct overflights, are clearly needed to continue assessing the accuracy of the radar-derived accumulation rates ~~from the layers within the firn over the GrIS~~.

The work shown here only incorporates layering detected in the radar data that is annual and continuously~~-~~ dated from the surface to depth at some location. ~~It does not~~We did not exhaustively trace all layering detected by the Snow Radar, i.e., there are still contiguous layers, not connected to a dated layer, in the dataset that were not utilized. For example, in the central-northern GrIS, there is a strongly reflecting layer varying between 15 and 18 m that cannot be dated with the radar data alone. If ice cores were drilled to identify this layer, techniques similar to those developed by MacGregor et al. (2015) or Das et al. (2015) could be used to determine multi-annual accumulation rates in additional regions of the GrIS and

Formatted: Font: Not Bold

Formatted: Font: Not Bold

extend the Snow Radar record. Additionally, furtherFurther deconvolution processing of the radar data, currently ongoing at CReSIS, will also resolves additional deeper layers in the Snow Radar data that will expand accumulation measurements in the future.

Annual-radar-derived accumulation rates are not extrapolated spatially here, due to their relative sparseness. Spatial extrapolation between the constantly varying flightlines, which vary in position from year-to-year, will bemust be left for future work, as additional data are collected and made available to fill in gaps.

In 2010 the largest overall discrepancy is evident between radar-derived and MAR estimates of accumulation. It does appear the MAR is overestimating accumulation over the southeastern GrIS in this year (Figure 10) and previous studies (Burgess et al., 2010) show that modeling accumulation is difficult in this region. However, the discrepancy is also due, at least in part, to the fact that in 2010 there is a higher percentage of radar data collected over the lower portions of the southeastern GrIS compared to other regions. This spatial sampling bias is amplifying the discrepancy in 2010. Because OIB data is not spatially consistent from year to year caution must be used when extrapolating to ice sheet scales.

In 2011 MAR appears to underestimate accumulation over the northwestern GrIS in a region just to the south of Camp Century. This small region is known to receive higher accumulation locally than the surrounding areas as storms on the west coast are diverted as the land mass to the north protrudes farther west into Baffin Bay (K. Steffen, personal communication). MAR does show increased accumulation in this region (Figure 5), however, not to the same magnitude as the radar-derived measurements. It is possible that MAR not estimating the magnitude of this relatively local high in precipitation due to it close proximity to the lateral boundaries where the larger resolution GCM may not completely capture the phenomena. This emphasizes the importance of understanding the possible effects of lateral forcing of RCM on accumulation fields and warrants further study.

Finally, the largest uncertainty in the radar-derived accumulation rate comes from the hybrid measured-modelled density profiles used. Spatially distributed density measurements and improved density models spanning the entire firn column are required to take full advantage of the layering detected by near-surface radars and to reduce the errors in radar-derived accumulation rates. More specifically, as shown in Figure 1, theThe current sampling of in situ measurements has large spatial gaps over the southwestern, north and and northeastern GrIS and the majority of the measurements are located in the upper-percolation and dry-snow zones (Figure 1). To further constrain and improve the density models required for radar-derived accumulation rates, these ~~spatial~~ gaps ~~and sampling distributions~~must be filled ~~and broaden~~ with additional measurements. Additionally, the Snow Radar's signal penetration around the perimeter of the GrIS is relatively shallow, resolving 1 to 3 annual layers only, with the majority of detected layers in the top meter of snow/firn (Figures 6 and 7). Accumulation rates are calculated using measurement averages in this section of the snow/firn column, likely causing less error than the MAR-modeled density. Improvement to modeled near-surface density should be considered for improved Snow Radar analysis.

Formatted: Indent: First line: 0"

7 Conclusions

A semi-automated method was developed to process tens of thousands of kilometers of airborne Snow Radar data collected by OIB across the GrIS between 2009 and 2012. The resulting radar-derived accumulation-rate dataset represents the largest validation dataset for recent annual accumulation rates across the GrIS to date. This dataset captures the large-scale accumulation-rate patterns of the GrIS well. Over two decades of annual radiostratigraphy is observed in the dry snow zone, near Summit Station, and 1 to 3 years are generally detectable in the ablation/percolation zones. Our estimated uncertainty in the radar-derived accumulation is 12~~0~~%, with the largest error contribution coming from the hybrid measured-modelled density profiles. This study emphasizes the need for ice cores coincident in time with airborne overflights and, more importantly, for improved density profiles, particularly in the top 1 m of snow/firn. These radar-derived accumulation-rate datasets should be used to evaluate RCM/GCM and reanalysis products, as demonstrated here using the MAR model. MAR ~~reproduces~~ matches the radar-derived accumulation rates well for most of the interior of the GrIS, but tends to overestimate accumulation rates in the southeastern coastal region of the GrIS and, in at least one year, underestimates accumulation rates in the northwestern costal region of the GrIS. While determining the precise nature of these differences is left for future work, we have clearly demonstrated the usefulness of the ice-sheet-wide, radar-derived accumulation-rate datasets for improving SMB estimates. As the GrIS continues to lose mass through SMB processes, monitoring accumulation rates directly is vital.

Acknowledgements

This work was supported by the NASA Cryospheric Sciences Program and by the NSF grant #1304700 and the NASA grants #NNX15AL45G and #NNX14AD98G. Data collection and instrument development were made possible by The University of Kansas' Center for Remote Sensing of Ice Sheets (CReSIS) supported by the National Science Foundation and NASA's Operation IceBridge. Publication of this article was funded by the University of Colorado Boulder Libraries Open Access Fund.

References

Alexander, P. M., Tedesco, M., Fettweis, X., van de Wal, R. S. W., Smeets, C. J. P. P. and van den Broeke, M. R.: Assessing spatio-temporal variability and trends in modelled and measured Greenland Ice Sheet albedo (2000–2013), The Cryosphere, 8(6), 2293–2312, doi:10.5194/tc-8-2293-2014, 2014.

Alley, R. B., Saltzman, E. S., Cuffey, K. M. and Fitzpatrick, J. J.: Summertime formation of Depth Hoar in central Greenland, Geophys. Res. Lett., 17(13), 2393–2396, doi:10.1029/GL017i013p02393, 1990.

Anschütz, H., Steinhage, D., Eisen, O., Oerter, H., Horwath, M. and Ruth, U.: Small-scale spatio-temporal characteristics of accumulation rates in western Dronning Maud Land, Antarctica, Journal of Glaciology, 54(185), 315–323, doi:10.3189/002214308784886243, 2008.

Arcone, S. A., Spikes, V. B. and Hamilton, G. S.: Phase structure of radar stratigraphic horizons within Antarctic firn, Annals of Glaciology, 41(1), 10–16, doi:10.3189/172756405781813267, 2005.

Benson, C. S.: Stratigraphic studies in the snow and firn of the Greenland Ice sheet, SIPRE Res. Rep., 70, 1962.

Baker, I. Density and permeability measurements with depth for the NEEM 2009S2 firn core. ACADIS Gateway, accessed 2015.

van den Broeke, M., Bamber, J., Ettema, J., Rignot, E., Schrama, E., Berg, W. J. van de, Meijgaard, E. van, Velicogna, I. and Wouters, B.: Partitioning Recent Greenland Mass Loss, Science, 326(5955), 984–986, doi:10.1126/science.1178176, 2009.

Brun, E., David, P., Sudul, M. and Brunot, G.: A numerical model to simulate snow-cover stratigraphy for operational avalanche forecasting, Journal of Glaciology, 38, 13–22, 1992.

Burgess, E. W., Forster, R. R., Box, J. E., Mosley-Thompson, E., Bromwich, D. H., Bales, R. C. and Smith, L. C.: A spatially calibrated model of annual accumulation rate on the Greenland Ice Sheet (1958–2007), J. Geophys. Res., 115(F2), F02004, doi:10.1029/2009JF001293, 2010.

Chen, L., Johannessen, O. M., Wang, H.. and Ohmura, A.: Accumulation over the Greenland Ice Sheet as represented in reanalysis data, Adv. Atmos. Sci., 28(5), 1030–1038, doi:10.1007/s00376-010-0150-9, 2011.Colgan, W., Box, J. E., Andersen, M. L., Fettweis, X., Csathó, B., Fausto, R. S., Van As, D. and Wahr, J.: Greenland high-elevation mass balance: inference and implication of reference period (1961–90) imbalance, Annals of Glaciology, 56(70), 105–117, doi:10.3189/2015AoG70A967, 2015.

Cullather, R. I. and Bosilovich, M. G.: The Energy Budget of the Polar Atmosphere in MERRA, Journal of Climate, 25(1), 5–24, doi:10.1175/2011JCLI4138.1, 2012.

Cullather, R. I., Nowicki, S. M., Zhao, B. and Suarez, M. J.: Evaluation of the surface representation of the Greenland Ice Sheet in a general circulation model, Journal of Climate, 27(13), 4835–4856, 2014.

Das, I., Scambos, T. A., Koenig, L. S., van den Broeke, M. R. and Lenaerts, J. T. M.: Extreme wind-ice interaction over Recovery Ice Stream, East Antarctica, Geophys. Res. Lett., 42(19), 2015GL065544, doi:10.1002/2015GL065544, 2015.

Dee, D. P., Uppala, S. M., Simmons, A. J., Berrisford, P., Poli, P., Kobayashi, S., Andrae, U., Balmaseda, M. A., Balsamo, G., Bauer, P., Bechtold, P., Beljaars, A. C. M., van de Berg, L., Bidlot, J., Bormann, N., Delsol, C., Dragani, R., Fuentes, M., Geer, A. J., Haimberger, L., Healy, S. B., Hersbach, H., Hólm, E. V., Isaksen, L., Kållberg, P., Köhler, M., Matricardi, M., McNally, A. P., Monge-Sanz, B. M., Morcrette, J.-J., Park, B.-K., Peubey, C., de Rosnay, P., Tavolato, C., Thépaut, J.-N. and Vitart, F.: The ERA-Interim reanalysis: configuration and performance of the data assimilation system, Quarterly Journal of the Royal Meteorological Society, 137(656), 553–597, doi:10.1002/qj.828, 2011.

Dibb, J. E. and Fahnestock, M.: Snow accumulation, surface height change, and firn densification at Summit, Greenland: Insights from 2 years of in situ observation, J. Geophys. Res., 109(D24), D24113, doi:10.1029/2003JD004300, 2004.

Enderlin, E. M., Howat, I. M., Jeong, S., Noh, M.-J., van Angelen, J. H. and van den Broeke, M. R.: An improved mass budget for the Greenland ice sheet, Geophys. Res. Lett., 41(3), 2013GL059010, doi:10.1002/2013GL059010, 2014.

Ettema, J., van den Broeke, M. R., van Meijgaard, E., van de Berg, W. J., Bamber, J. L., Box, J. E. and Bales, R. C.: Higher surface mass balance of the Greenland ice sheet revealed by high-resolution climate modeling, Geophys. Res. Lett., 36(12), L12501, doi:10.1029/2009GL038110, 2009.

Fettweis, X.: Reconstruction of the 1979–2006 Greenland ice sheet surface mass balance using the regional climate model MAR, The Cryosphere, 1(1), 21–40, doi:10.5194/tc-1-21-2007, 2007.

Fettweis, X., Gallée, H., Lefebre, F. and Ypersele, J.-P. van: Greenland surface mass balance simulated by a regional climate model and comparison with satellite-derived data in 1990–1991, Climate Dynamics, 24(6), 623–640, doi:10.1007/s00382-005-0010-y, 2005.

Fettweis, X., Tedesco, M., van den Broeke, M. and Ettema, J.: Melting trends over the Greenland ice sheet (1958–2009) from spaceborne microwave data and regional climate models, The Cryosphere, 5(2), 359–375, doi:10.5194/tc-5-359-2011, 2011.

Fettweis, X., Franco, B., Tedesco, M., van Angelen, J. H., Lenaerts, J. T. M., van den Broeke, M. R. and Gallée, H.: Estimating the Greenland ice sheet surface mass balance contribution to future sea level rise using the regional atmospheric climate model MAR, The Cryosphere, 7(2), 469–489, doi:10.5194/tc-7-469-2013, 2013.

~~Fowler, N. O., McCall, D., Chou, T. C., Holmes, J. C. and Hanenson, I. B.: Electrocardiographic changes and cardiac arrhythmias in patients receiving psychotropic drugs, Am. J. Cardiol., 37(2), 223–230, 1976.~~

Gallée, H.: Air-sea interactions over Terra Nova Bay during winter: Simulation with a coupled atmosphere-polynya model, J. Geophys. Res., 102(D12), 13835–13849, doi:10.1029/96JD03098, 1997.

Gallée, H. and Schayes, G.: Development of a Three-Dimensional Meso-γ Primitive Equation Model: Katabatic Winds Simulation in the Area of Terra Nova Bay, Antarctica, Mon. Wea. Rev., 122(4), 671–685, doi:10.1175/1520-0493(1994)122<0671:DOATDM>2.0.CO;2, 1994.

Gubler, H. and Hiller, M.: The use of microwave FMCW radar in snow and avalanche research, Cold Regions Science and Technology, 9(2), 109–119, doi:10.1016/0165-232X(84)90003-X, 1984.

Hanna, E., Huybrechts, P., Cappelen, J., Steffen, K., Bales, R. C., Burgess, E., McConnell, J. R., Peder Steffensen, J., Van den Broeke, M., Wake, L., Bigg, G., Griffiths, M. and Savas, D.: Greenland Ice Sheet surface mass balance 1870 to 2010 based on Twentieth Century Reanalysis, and links with global climate forcing, J. Geophys. Res., 116(D24), D24121, doi:10.1029/2011JD016387, 2011.

Hawley, R. L., Morris, E. M., Cullen, R., Nixdorf, U., Shepherd, A. P. and Wingham, D. J.: ASIRAS airborne radar resolves internal annual layers in the dry-snow zone of Greenland, Geophys. Res. Lett., 33(4), L04502, doi:10.1029/2005GL025147, 2006.

Hawley, R. L., Courville, Z. R., Kehrl, L. M., Lutz, E. R., Osterberg, E. C., Overly, T. B. and Wong, G. J.: Recent accumulation variability in northwest Greenland from ground-penetrating radar and shallow cores along the Greenland Inland Traverse, Journal of Glaciology, 60, 375–382, doi:10.3189/2014JoG13J141, 2014.

Kanagaratnam, P., Gogineni, S. P., Gundestrup, N. and Larsen, L.: High-resolution radar mapping of internal layers at the North Greenland Ice Core Project, Journal of Geophysical Research, 106(D24), 33799, doi:10.1029/2001JD900191, 2001.

Kanagaratnam, P., Gogineni, S. P., Ramasami, V. and Braaten, D.: A wideband radar for high-resolution mapping of near-surface internal layers in glacial ice, IEEE Transactions on Geoscience and Remote Sensing, 42(3), 483–490, doi:10.1109/TGRS.2004.823451, 2004.

Koenig, L., Box, J. and Kurtz, N.: Improving Surface Mass Balance Over Ice Sheets and Snow Depth on Sea Ice, Eos Trans. AGU, 94(10), 100–100, doi:10.1002/2013EO100006, 2013.

Koenig, L., Forster, R., Brucker, L. and Miller, J.: Remote sensing of accumulation over the Greenland and Antarctic ice sheets, in Remote Sensing of the Cryosphere, edited by M. Tedesco, pp. 157–186, John Wiley & Sons, Ltd., 2015.

Koenig, L., S. Martin, M. Studinger, and J. Sonntag: Polar Airborne Observations Fill Gap in Satellite Data, Eos Trans. AGU, 91(38), 333–334, doi:10.1029/2010EO380002, 2010.

Koenig, L. S., Miège, C., Forster, R. R. and Brucker, L.: Initial in situ measurements of perennial meltwater storage in the Greenland firn aquifer, Geophys. Res. Lett., 41(1), 2013GL058083, doi:10.1002/2013GL058083, 2014.

Koenig, L and the Surface mass balance and snow on sea ice working group (SUMup). SUMup Snow Density Dataset. Greenbelt, MD, USA: NASA Goddard Space Flight Center. Digital media, accessed 2015.

Krabill, W., Hanna, E., Huybrechts, P., Abdalati, W., Cappelen, J., Csatho, B., Frederick, E., Manizade, S., Martin, C., Sonntag, J., Swift, R., Thomas, R. and Yungel, J.: Greenland Ice Sheet: Increased coastal thinning, Geophys. Res. Lett., 31(24), L24402, doi:10.1029/2004GL021533, 2004.

Lefebre, F.: Modeling of snow and ice melt at ETH Camp (West Greenland): A study of surface albedo, Journal of Geophysical Research, 108(D8), doi:10.1029/2001JD001160, 2003.

Legarsky, J. J.: Synthetic-aperture radar (SAR) processing of glacial ice depth-sounding data, ka-band backscattering measurements and applications (Doctoral dissertation). Retrieved from ProQuest Dissertations Publishing. (9946109), 1999.

Leuschen, C.: IceBridge Snow Radar L1B Geolocated Radar Echo Strength Profiles, Boulder, Colorado, NASA DAAC at the National Snow and Ice Data Center, http://dx.doi.org/10.5067/FAZTWP500V70, accessed 2014.

Looyenga, H.: Dielectric constants of heterogeneous mixtures, Physica, 31, 401–406, doi:10.1016/0031-8914(65)90045-5, 1965.

MacGregor, J. A., Fahnestock, M. A., Catania, G. A., Paden, J. D., Prasad Gogineni, S., Young, S. K., Rybarski, S. C., Mabrey, A. N., Wagman, B. M. and Morlighem, M.: Radiostratigraphy and age structure of the Greenland Ice Sheet, J. Geophys. Res. Earth Surf., 120(2), 2014JF003215, doi:10.1002/2014JF003215, 2015.

MacGregor, J. A., W. T. Colgan, M. A. Fahnestock, M. Morlighem, G. A. Catania, J. D. Paden and S. P. Gogineni, Holocene deceleration of the Greenland Ice Sheet, Science, 351 , 590–593, doi:10.1126/science.aab1702, 2016.

Marshall, H.-P. and Koh, G.: FMCW radars for snow research, Cold Regions Science and Technology, 52(2), 118–131, 2008.

Schneebeli, M. Coléou, C., Touvier, F. and Lesaffre, B.: Measurement of density and wetness in snow using time-domain reflectometry, Annals of Glaciology, 26, 1998.

Medley, B., Joughin, I., Das, S. B., Steig, E. J., Conway, H., Gogineni, S., Criscitiello, A. S., McConnell, J. R., Smith, B. E., van den Broeke, M. R., Lenaerts, J. T. M., Bromwich, D. H. and Nicolas, J. P.: Airborne-radar and ice-core observations of annual snow accumulation over Thwaites Glacier, West Antarctica confirm the spatiotemporal variability of global and regional atmospheric models, Geophys. Res. Lett., 40(14), 3649–3654, doi:10.1002/grl.50706, 2013.

Miège, C., Forster, R. R., Box, J. E., Burgess, E. W., McConnell, J. R., Pasteris, D. R. and Spikes, V. B.: Southeast Greenland high accumulation rates derived from firn cores and ground-penetrating radar, Annals of Glaciology, 54(63), 322–332, doi:10.3189/2013AoG63A358, 2013.

Mosley-Thompson, E., McConnell, J. R., Bales, R. C., Li, Z., Lin, P.-N., Steffen, K., Thompson, L. G., Edwards, R. and Bathke, D.: Local to regional-scale variability of annual net accumulation on the Greenland ice sheet from PARCA cores, J. Geophys. Res., 106(D24), 33839–33851, doi:10.1029/2001JD900067, 2001.

Müller, K., Sinisalo, A., Anschütz, H., Hamran, S.-E., Hagen, J.-O., McConnell, J. R. and Pasteris, D. R.: An 860 km surface mass-balance profile on the East Antarctic plateau derived by GPR, Annals of Glaciology, 51(55), 1–8, doi:10.3189/172756410791392718, 2010.

Nghiem, S. V., Steffen, K., Neumann, G. and Huff, R.: Mapping of ice layer extent and snow accumulation in the percolation zone of the Greenland ice sheet, J. Geophys. Res., 110(F2), F02017, doi:10.1029/2004JF000234, 2005.

~~Onana, V., Koenig, L. S., Ruth, J., Studinger, M. and Harbeck, J. P.: A Semiautomated Multilayer Picking Algorithm for Ice-Sheet Radar Echograms Applied to Ground-Based Near-Surface Data, IEEE Transactions on Geoscience and Remote Sensing, 53(1), 51–69, doi:10.1109/TGRS.2014.2318208, 2015.~~

Panzer, B., Gomez-Garcia, D., Leuschen, C., Paden, J., Rodriguez-Morales, F., Patel, A., Markus, T., Holt, B. and Gogineni, P.: An ultra-wideband, microwave radar for measuring snow thickness on sea ice and mapping near-surface internal layers in polar firn, Journal of Glaciology, 59(214), 244–254, doi:10.3189/2013JoG12J128, 2013.

de la Peña, S., Nienow, P., Shepherd, A., Helm, V., Mair, D., Hanna, E., Huybrechts, P., Guo, Q., Cullen, R. and Wingham, D.: Spatially extensive estimates of annual accumulation in the dry snow zone of the Greenland Ice Sheet determined from radar altimetry, The Cryosphere, 4(4), 467–474, doi:10.5194/tc-4-467-2010, 2010.

Rodriguez-Morales, F., Gogineni, S., Leuschen, C. J., Paden, J. D., Li, J., Lewis, C. C., Panzer, B., Gomez-Garcia Alvestegui, D., Patel, A., Byers, K., Crowe, R., Player, K., Hale, R. D., Arnold, E. J., Smith, L., Gifford, C. M., Braaten, D. and Panton, C.: Advanced Multifrequency Radar Instrumentation for Polar Research, IEEE Transactions on Geoscience and Remote Sensing, 52(5), 2824–2842, doi:10.1109/TGRS.2013.2266415, 2014.

Shepherd, A., Ivins, E. R., A, G., Barletta, V. R., Bentley, M. J., Bettadpur, S., Briggs, K. H., Bromwich, D. H., Forsberg, R., Galin, N., Horwath, M., Jacobs, S., Joughin, I., King, M. A., Lenaerts, J. T. M., Li, J., Ligtenberg, S. R. M., Luckman, A., Luthcke, S. B., McMillan, M., Meister, R., Milne, G., Mouginot, J., Muir, A., Nicolas, J. P., Paden, J., Payne, A. J., Pritchard, H., Rignot, E., Rott, H., Sørensen, L. S., Scambos, T. A., Scheuchl, B., Schrama, E. J. O., Smith, B., Sundal, A. V., Angelen, J. H. van, Berg, W. J. van de, Broeke, M. R. van den, Vaughan, D. G., Velicogna, I., Wahr, J., Whitehouse, P. L., Wingham, D. J., Yi, D., Young, D. and Zwally, H. J.: A Reconciled Estimate of Ice-Sheet Mass Balance, Science, 338(6111), 1183–1189, doi:10.1126/science.1228102, 2012.

Spikes, V. B., Hamilton, G. S., Arcone, S. A., Kaspari, S. and Mayewski, P. A.: Variability in accumulation rates from GPR profiling on the West Antarctic plateau, Annals of Glaciology, 39(1), 238–244, doi:10.3189/172756404781814393, 2004.

Tedesco, M.,Box, J. E., Cappelen, J., Fausto, R. S, Fettweis, X., Hansen, K., Mote, T., Smeets, C.J.P.P., van As, D., van de Wal, R.S.W. and Wahr, J.: Greenland Ice Sheet. In Arctic Report Card: Update for 2015, http://www.arctic.noaa.gov/reportcard/greenland_ice_sheet.html, 2015.

Tiuri, M. E., Sihvola, A. H., Nyfors, E. and Hallikaiken, M.: The complex dielectric constant of snow at microwave frequencies, IEEE Journal of Oceanic Engineering, 9(5), 377–382, doi:10.1109/JOE.1984.1145645, 1984.

Vernon, C. L., Bamber, J. L., Box, J. E., van den Broeke, M. R., Fettweis, X., Hanna, E. and Huybrechts, P.: Surface mass balance model intercomparison for the Greenland ice sheet, The Cryosphere, 7(2), 599–614, doi:10.5194/tc-7-599-2013, 2013.

Wiesmann, A. and Mätzler, C.: Microwave Emission Model of Layered Snowpacks, Remote Sensing of Environment, 70(3), 307–316, doi:10.1016/S0034-4257(99)00046-2, 1999.

Table 1: Radar-derived accumulation-rate crossover analysis. Columns include the year the radar data were collected, the number of, the mean, the standard deviation and the maximum difference of radar-derived accumulation at crossover points. Minimum crossover values were zero for all years. The final column shows the mean difference between the gridded-radar-derived accumulation and the MAR estimates of accumulation from July 1 to April 30.

Year	# of Crossovers	Mean Crossover in (m w.e. a^{-1} and (range bin))	Std. Crossover in (m w.e. a^{-1} and (range bin))	Max Crossovers in (m w.e. a^{-1} and (range bin))	Mean Difference Radar-MAR in (m w.e. a^{-1})
2009	21	0.03(5)	0.04(7)	0.12(23)	-0.05
2010	270	0.02(3)	0.02(5)	0.16(40)	-0.18
2011	992	0.04(3)	0.06(4)	0.60(59)	0.01
2012	579	0.04(5)	0.04(6)	0.31(39)	0.03

Formatted Table

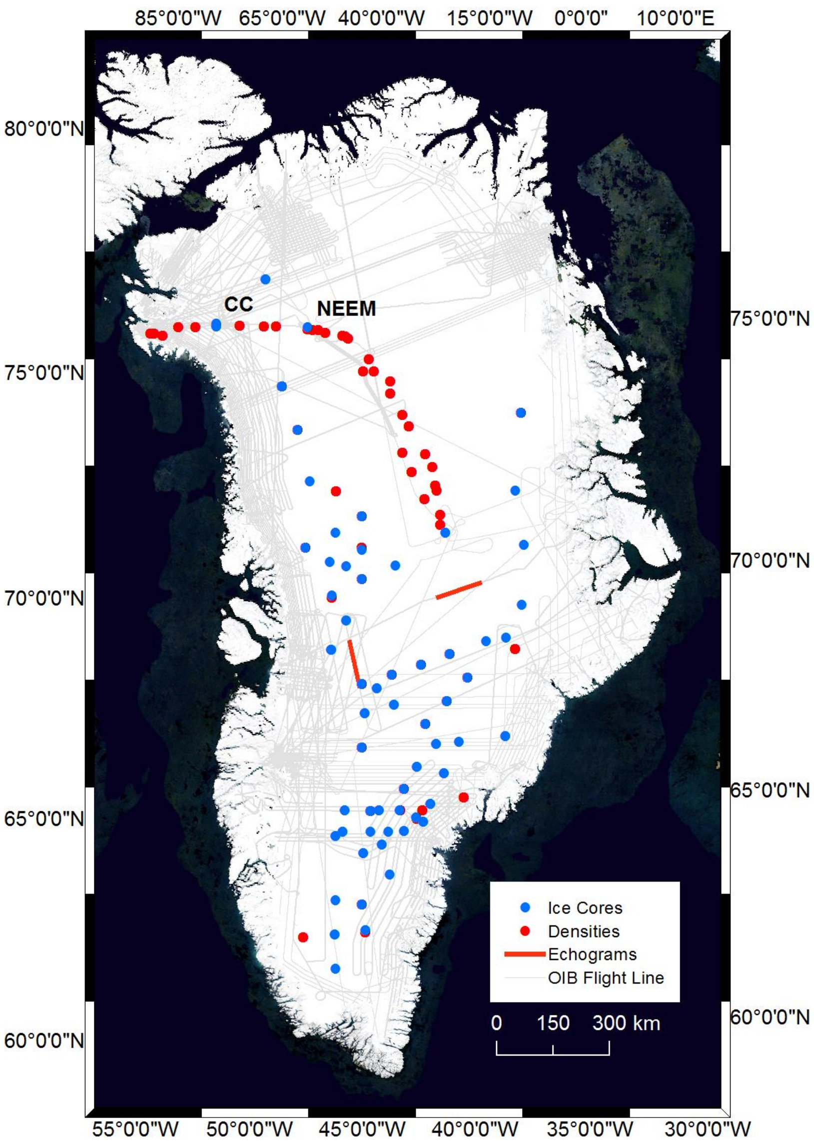

Figure 1: Locations of snow/firn density measurements (red circles) and ice core accumulation measurements (blue circles) used in this study with OIB flightline coverage from 2009 through 2012 (gray lines). Camp Century (CC) and NEEM core locations are labeled and the red lines indicate the locations of the radargrams in Figure 3.

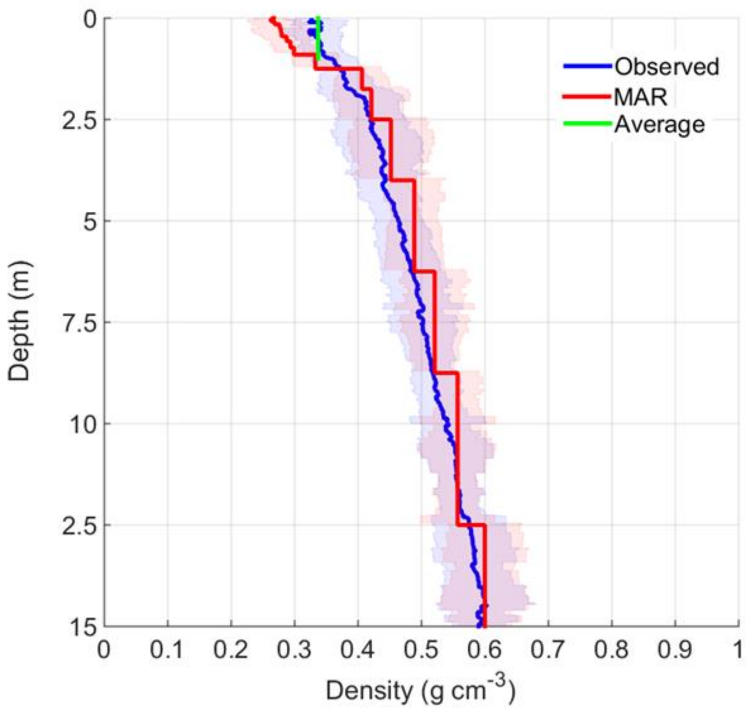

Figure 2: Mean observed (blue) and MAR modelled (red) densities profiles with one standard deviation (shaded regions) showing an underestimation of modelled densities in the top 1 m of snow/firn. The mean observed density in the top 1 m (green) was used with the modelled densities below to create a hybrid measured-modelled density profile. The locations of the density measurements are shown in Figure 1 and the measurements and modeled profiles are contemporaneous.

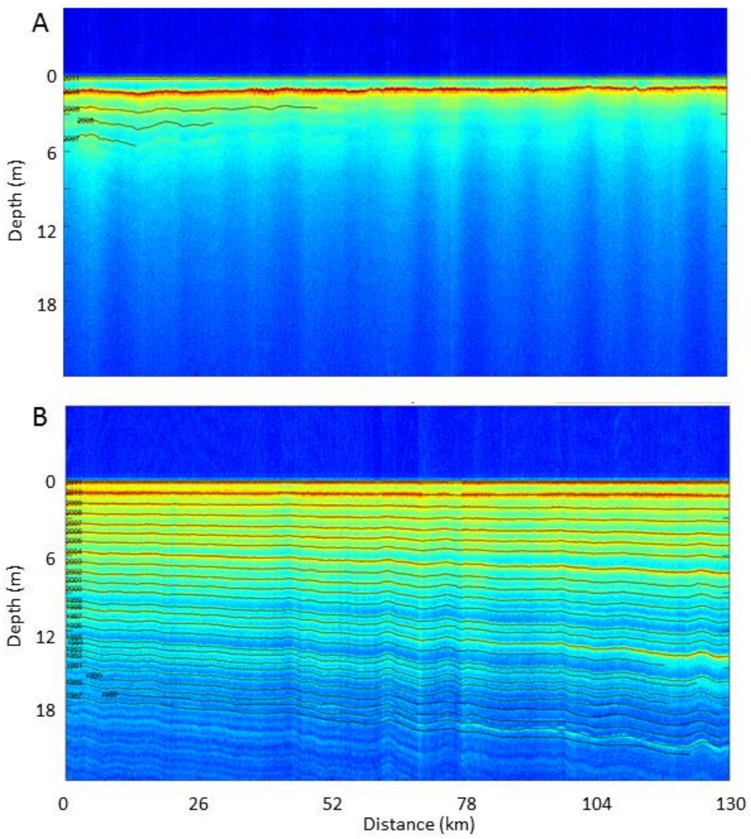

Figure 3: Example Snow Radar ~~echograms~~ radargrams from 2011 in the percolation zone (top), inland from Jakobshavn Isbræ, and dry snow zone (bottom), near the ice divide ~220 km south of Summit Station, showing automatically picked layers (black) resulting from the layer picking algorithm before any manual adjustments. Indexing by year is shown at the left end of each picked layer. Snow Radar data frames represented are 20110422_01_218 to 20110422_01_244 (top) and 20110426_03_155 to 20110426_03_180 (bottom) (Leuschen, 2014). Locations of the radargrams are shown by the red lines in Figure 1.

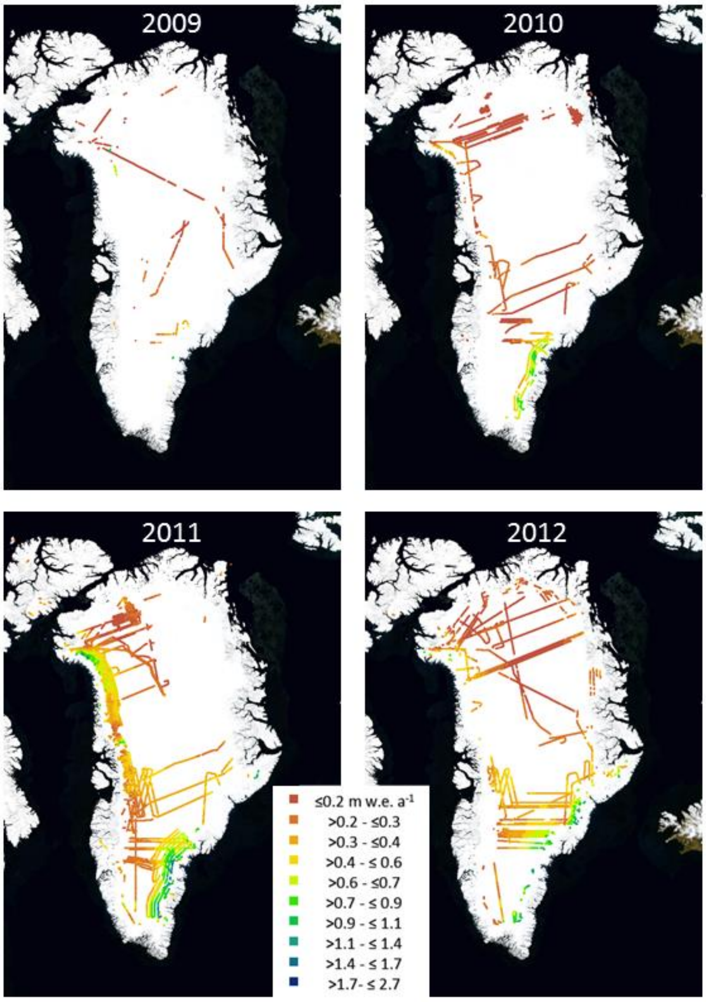

Figure 4: Radar-derived-annual accumulation rate (m w.e. a^{-1}) for 2009 through 2012 from Operation IceBridge Snow Radar data representing the top layer in each year (July 1 to April 30).

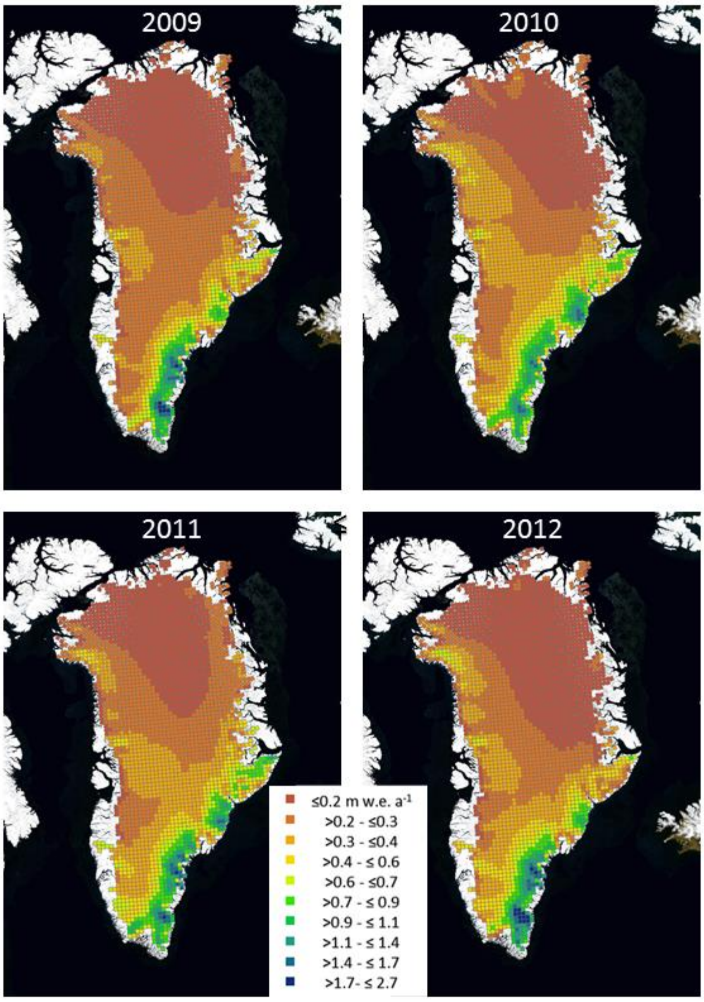

Figure 5: Modelled estimates of annual accumulation (m w.e. a^{-1}) over the GrIS for 2009 through 2012 from the Modèle Atmosphérique Régional (MAR) regional climate model (v3.5.2) (representing July 1 to April 30 to match the radar-derived estimates).

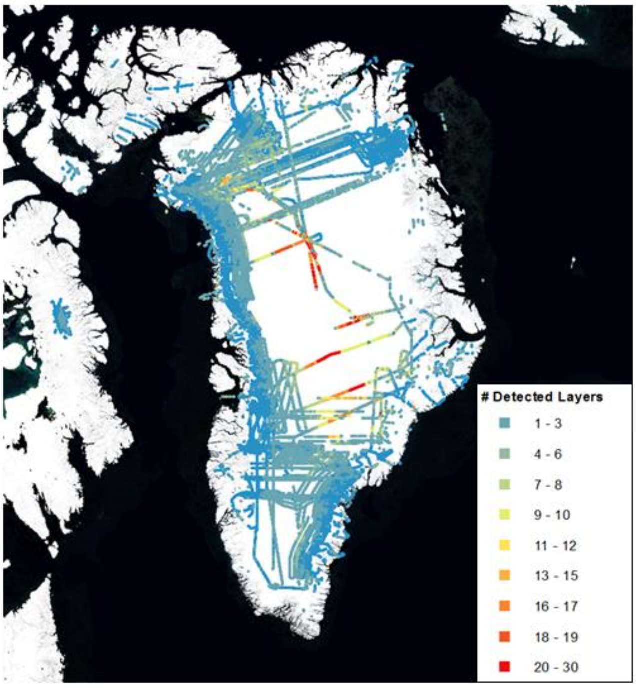

Figure 6: Number of detected annual layers from 2009 through 2012 showing that, for the majority of the GrIS, fewerless than three layers, or previous years of accumulation, were detected.

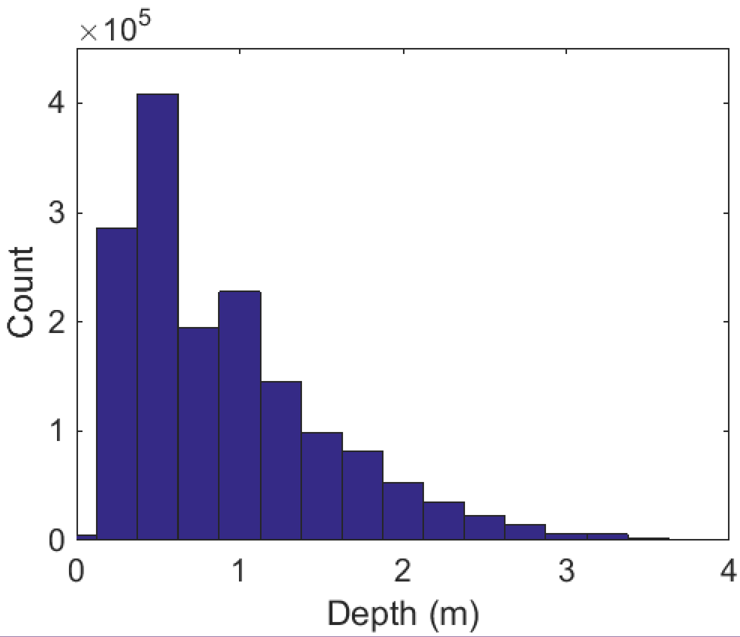

Figure 7: Histogram of first layer depth from 2009 through 2012 showing that the majority 63% of the first layer depths are within the top 1 m of snow.

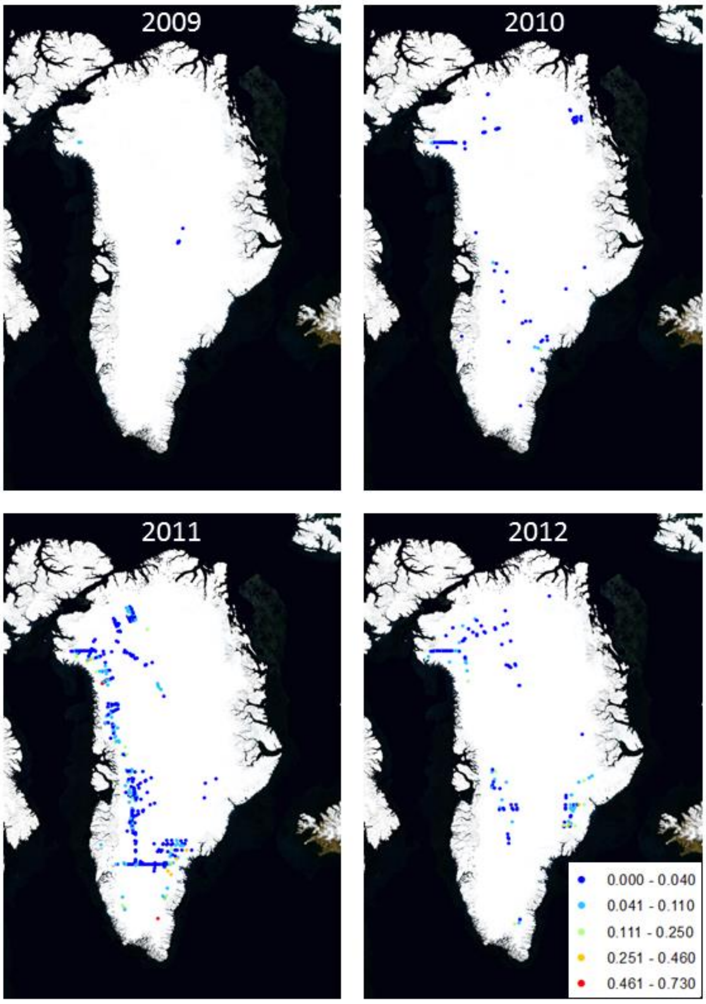

Figure 87: Maps of annual-crossover error (m w.e. a^{-1}) from the radar-derived accumulation for 2009 through 2012.

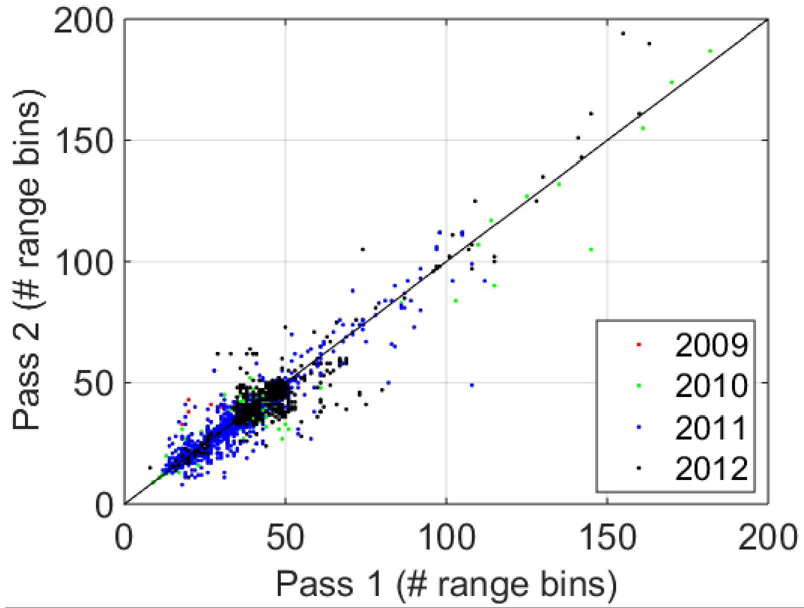

Figure 98: Crossover errors from the radar derived accumulation (m w.e.) from 2009 through 2012 in range bins. Figure 87 shows the spatial distribution of these crossover errors in (m w.e. a^{-1})..

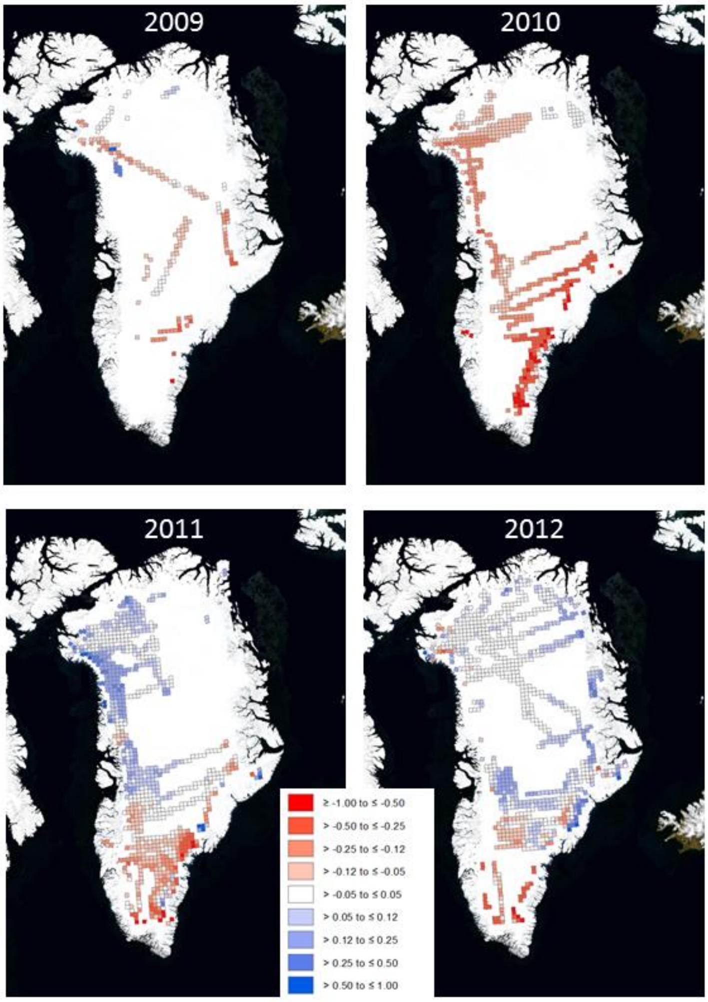

Figure 109: Difference between annual radar-derived and MAR-estimated accumulation rate (m w.e. a^{-1}) showing MAR overestimation in red and underestimation in blue.

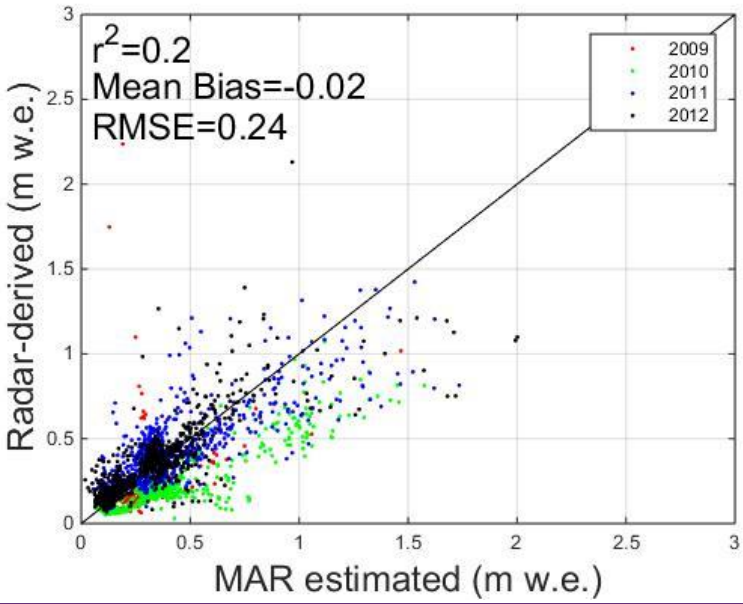

Figure 11~~0~~: Comparison between radar-derived and MAR-estimated accumulation rate (m w.e. a^{-1}). Radar-derived accumulations (Figure 4) were averaged within each MAR grid cell. Figure 9 shows the spatial distribution of the differences.

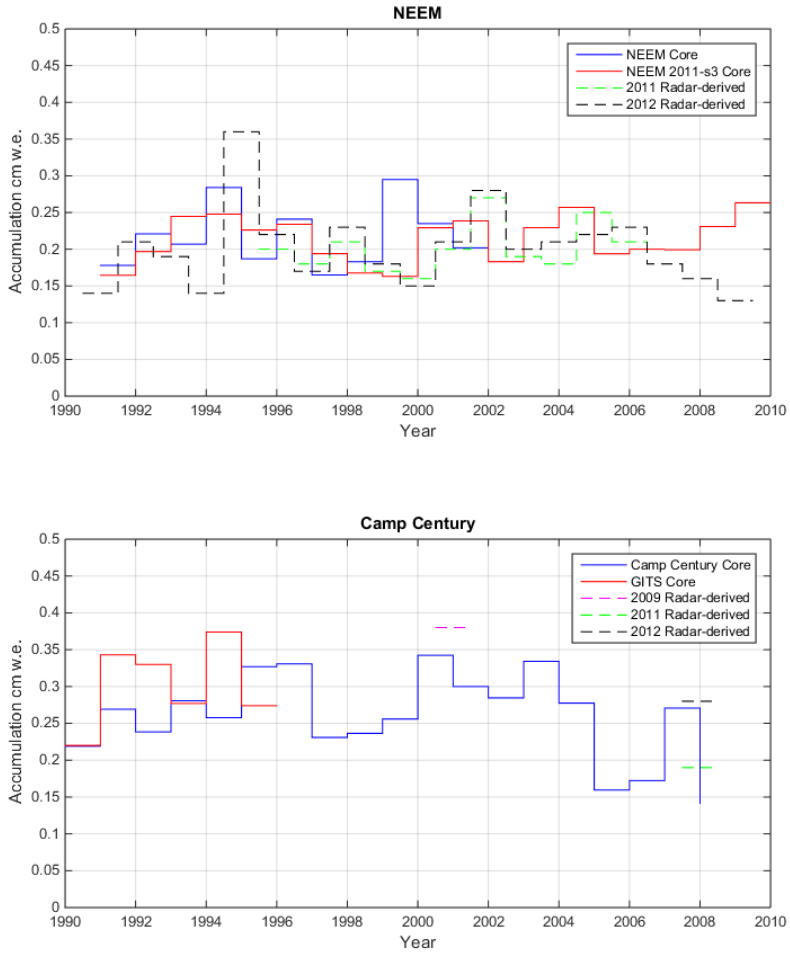

Figure 121: Annual accumulation rate measured from the two cores at both the NEEM and Camp Century locations compared to temporally overlapping radar-derived values.